DESIGN OF ACTIVE FILTER SYSTEMS USING PARAMETER PLANE TECHNIQUES.

by

Ronald Clement Funk

UNITED STATES
NAVAL POSTGRADUATE SCHOOL

THESIS

DESIGN OF ACTIVE FILTER SYSTEMS
USING PARAMETER PLANE TECHNIQUES

by

Ronald Clement Funk

December 1968

DESIGN OF ACTIVE FILTER SYSTEMS

USING PARAMETER PLANE TECHNIQUES

by

Ronald Clement Funk
Lieutenant, United States Navy
B.S.E.E., University of Oklahoma, 1962

Submitted in partial fulfillment of the
requirements for the degree of

MASTER OF SCIENCE IN ELECTRICAL ENGINEERING

from the

NAVAL POSTGRADUATE SCHOOL
December 1968

ABSTRACT

Since parameter planes were introduced, considerable investigation has been conducted in proving that the results obtained by this method are in agreement with those obtained from various other proven techniques. Research undertaken in this paper illustrates methods by which parameter planes are useful in the design of electrical networks. The investigations were conducted on an active parallel-T filter, in which the utilization of the constant bandwidth curves are beneficial, and the high Q double tuned filter, where constant zeta curves aided in the design.

TABLE OF CONTENTS

LIST OF ILLUSTRATIONS

1. INTRODUCTION

The mathematical bases for parameter plane analysis of systems are available in (1) and (2). Parameter plane techniques have been applied to the problem of analyzing the dynamic response of systems with some attention to compensation design. This thesis is concerned with the problem of implementing parameter plane procedures as a useful aid in the design of electrical networks. The purpose of this paper is to incorporate parameter planes in the design of actual circuits. These circuits have been selected to illustrate the varying degrees of assistance the utilization of parameter planes can provide.

2. PHILOSOPHY OF PARAMETER PLANES

In the design of certain electrical networks it would be advantageous to have available a procedure for determining the most satisfactory values of various circuit elements other than by trial and error. Preliminary studies have shown that parameter plane techniques give results that are in agreement with those obtained with other proven techniques. The parameter plane provides a family of curves where two of the variables are two of the circuit elements. Various families of curves are readily computed, each providing information about some chosen circuit characteristics as a function of the two variables. One curve which provides very beneficial information is the family of constant bandwidth curves. Here the two circuit elements are incorporated as the coordinate variables, and the resulting family of curves displays the values of these elements which result in a constant magnitude of the frequency response of the circuit. A second curve which is available for network design is the constant zeta curve. Here the family of curves represents the element values necessary to establish the desired value of zeta for a given network.

3. THE ACTIVE PARALLEL-T NETWORK

3.1. The active parallel-T network of figure 3-1 is one section of the RC elliptical function filter designed by NASA's Ames Laboratory. Mr. Nakagawa in his thesis (3) uses this network to show that the results obtained by parameter plane techniques are in agreement with known experimental results. Utilizing this network, two specific configurations will be examined for the application of parameter planes in their design.

3.2. From (3), the transfer function T(s) for this network was shown to be:

$$T(s) = \frac{K(p^2 + 1)}{p^2 + \left[(k+1)/k\right]\left[2 + \left(\frac{kR}{Z}\right)\right] p + 1 + \left[(k+1)/Z\right] R} \qquad (3\text{-}1)$$

where p = RCs, thus normalizing the transfer function to 1. Since p could then be considered to have assumed the role of s, substituting $p = j\omega$ into T(s) and plotting the frequency response resulted in the magnitude of T(s) being identically zero (or minus infinity in db) at $\omega = 1$, the 'notch frequency', f_n. This notch frequency could then be adjusted as desired by using the relationship:

$$f_n = 1/2\pi RC \qquad (3\text{-}2)$$

3.3. For the first configuration, a capacitance 'C_z' will be incorporated as the load impedance 'Z'.

Substituting $Z = 1/C_z s$ into equation 3-1:

$$T(s) = \frac{K(p^2 + 1)}{p^2 + \left[(k+1)/k\right]\left[2 + kRC_z s - K\right]p + 1 + (k+1)RC_z s}$$

now let $C_z = C'C$, then:

$$T(s) = \frac{K(p^2 + 1)}{p^2 + \left[(k+1)/k\right]\left[2 + kC'RCs - K\right]p + 1 + (k+1)C'RCs}$$

since $p = RCs$:

$$T(s) = \frac{K(p^2 + 1)}{p^2 + \left[(k+1)/k\right]\left[2 + kC'p - K\right]p + 1 + (k+1)C'p}$$

$$T(s) = \frac{K(p^2 + 1)}{\left[1 + (k+1)C'\right]p^2 + \left[\left((k+1)/k\right)(2-K) + (k+1)C'\right]p + 1} \qquad (3\text{-}3)$$

Since parameter planes provide for two circuit parameters being variable, it is necessary to designate which of the three elements present in equation 3-3, amplifier gain 'K', normalized capacitance "C'", and component ratio 'k' should be made the variables, alpha and beta. For the normalized transfer function, the two zeros are always located at plus and minus one on the omega axis; therefore, the poles will be examined to determine the alpha and beta variables. Since the coefficients of the p^2 term and the constant term are always positive, the coefficient of the p term must be greater than or equal to zero to insure stability.

Applying this criterion:

$$\left[(k+1)/k\right]\left[2 - K\right] + (k+1)C' \geq 0 \qquad (3\text{-}4)$$

or rearranging:

$$K \leq 2 + kC' \qquad (3\text{-}5)$$

From equation 3-4, observe that the amplifier gain 'K' is preceded by a negative sign making the selection of its value very critical for system stability. It will therefore be designated as the variable parameter, alpha. The selection of the component ratio 'k' or the normalized capacitance "C'" as the second parameter variable have equal merit when equation 3-5 is examined. However, since the normalized capacitance "C'" has a direct relationship to the primary capacitance 'C', it will be designated as the variable parameter, beta. These two selections also correspond to those of Mr. Nakagawa's in (3).

3.4. Figures 3-2 and 3-3 represent examples of the many families of frequency response curves which can be formulated for this network configuration. For both figures, the component ratio 'k' and the normalized capacitance "C'" have been kept constant while the amplifier gain 'K' has been varied to produce the eight observed curves.

A further examination of figure 3-3 indicates that the portion of the frequency response between omega = 0.3 and omega = 0.9 is in fact similar to the response expected of a second order system with a pair of complex conjugate poles.

By evaluating the individual curves, it appears that the damping, zeta, is approaching zero when K = 3.2. Using the values of k = 3.0 and C' = 0.4 with K = 3.2 it is found that:

$$\left[(k+1)C'+ 1\right] p^2 + \left\{\left[(k+1)/k\right]\left[2-K\right] + (k+1)C'\right\}p+1 = 2.6p^2+1$$

which verifies that the damping is indeed zero at K = 3.2. By substituting $p = j\omega$, it is found that this occurs when the natural frequency is:

$$\omega_n = \sqrt{1/2.6} = .62 \text{ radians}$$

With this information, the desired frequency response can be specified.

For further illustration, it will be assumed that the desired response occurs when:

amplifier gain 'K' = 2.4

component ratio 'k' = 3.0

normalized capacitance "C'" = 0.4

These values have been extrapolated from figure 3-3.

3.5. Figures 3-4 through 3-10 are the constant bandwidth curves to be utilized in conjunction with figure 3-3. For each figure, the component ratio 'k' has been kept constant at 3.0 and each graph represents the constant bandwidth curves for a particular value of omega. The utilization of parameter planes has now allowed the amplifier gain 'K' to be the ordinate variable and the normalized capacitance "C'"

to be varied along the abcissa. The separation between consecutive bandwidth curves has been maintained at a constant 2db.

From figure 3-3, the region between omega = 0.4 and omega = 0.8 would be considered the most sensitive to the network's component values since the magnitude of the individual curves varies considerably in this area. This can be readily verified on the constant bandwidth curves by utilizing the selected operating values designated as point A on figures 3-4 through 3-10. From figure 3-4, the graph representing omega = 0.4, point A is located where the constant 6.85db curve would appear. To remain within a magnitude of plus or minus 1db, the amplifier gain can vary over the range of 2.25 to 2.55 when interpreting the range marked on the ordinate axis. Similarly, from figure 3-5, omega = 0.6, the increased sensitivity can readily be noted since the amplifier gain "K" is now limited to the range of 2.32 to 2.48 to achieve the same tolerance of a plus or minus 1db deviation in magnitude. This range is the same for omega = 0.65, figure 3-6, but then gradually increases again as omega increases, i.e.:

Omega = 0.8 $\quad 2.29 < K < 2.51$

Omega = 0.95 $\quad 2.25 < K < 2.55$

Omega = 1.05 $\quad 2.21 < K < 2.59$

Omega = 1.20 $\quad 2.19 < K < 2.61$

which are the graphs of figures 3-7 through 3-10.

The acceptable limits for the normalized capacitance "C'" can also be determined, but since the region of greatest sensitivity occurs in the area of omega = 0.60, only figure 3-5 will be utilized for this purpose. Here the normalized capacitance can vary between 0.37 and 0.43 and still be within the plus or minus 1db tolerance.

Since the preceeding determinations were conducted on one of the variables when the second was kept at its exact desired value, it is necessary to determine a maximum deviation of the two parameters as a combination. Using figure 3-5, it is seen that the normalized capacitance "C'" tolerance can be plus or minus 7.5 percent, and the amplifier gain "K" tolerance plus or minus 3.3 percent when considered individually. Therefore, when considered as a combination, allowing the amplifier gain "K" to vary from 2.33 to 2.47, approximately plus or minus 3 percent, and the normalized capacitance "C'" to vary from 0.375 to 0.425, plus or minus 5 percent, the maximum of a plus or minus 1db deviation in the magnitude of the frequency response can be maintained.

3.6. Having determined that the values of amplifier gain "K", component ratio "k", and normalized capacitance "C'" are acceptable, the values of the remaining network elements can readily be determined once the desired notch frequency is selected. For example, assume that the notch frequency is to be located at 1.59 KHZ. Then, with a value of R = 10 K ohms, and using equation 3-2;

$$C = 1/2\pi R\, f_n$$

$$C = 1/2\pi(10^4)(1.595)(10^3)$$

$$C = 0.01\mu \text{ farads}$$

Using these values of C and R and the desired component ratio, k = 3.0, the other network resistors and capacitors can now be calculated as follows:

$$C/k = 0.0033\mu \text{ farads}$$

$$\left((k+1)/k\right) C = 0.0133\mu \text{ farads}$$

$$kR = 30 \text{ Kohms}$$

$$\left(k/(k+1)\right) R = 7.5 \text{ Kohms}$$

The remaining element value to be determined is the load capacitor.

$$\text{From } C_z = C'C$$

$$C_z = (0.4)(0.01) = 0.004\mu \text{ farads}$$

Inserting all the component values in figure 3-1, the desired network is as shown in figure 3-1a.

3.7. For the second configuration, a resistance 'R_z' will be incorporated as the load impedance, Z. Substituting into the transfer function, T(s), equation 3-1 now becomes:

$$T(s) = \frac{K(p^2 + 1)}{p^2 + \left[(k+1)/k\right]\left[2 + kR/R_z - K\right] p + 1 + (k+1)R/R_z}$$

Letting $R/R_Z = R'$, where R' is defined as the normalized resistance, T(s) becomes:

$$T(s) = \frac{K(p^2 + 1)}{p^2 + \left[(k+1)/k\right]\left[2 + kR' - K\right] p + 1 + (k+1)R'}$$

or

$$T(s) = \frac{K(p^2 + 1)}{p^2 + \left[(k+1)/k\right]\left[2 - K\right]p + (k+1)R'p + 1 + (k+1)R'} \qquad (3\text{-}6)$$

To determine the two network elements which are to be the parameter plane variables, the same criteria used for the first configuration will be applied here. Again, the coefficients of the p^2 term and the constant term are always positive, so the coefficient of the p term must always be greater than or equal to zero for system stability. The application of this criterion to equation 3-6 yields:

$$(k + 1/k)(2 - K) + (k + 1)R' \geq 0 \qquad (3\text{-}7)$$

or:

$$K \leq 2 + kR' \qquad (3\text{-}8)$$

These two equations are identical to equations 3-4 and 3-5 except that the normalized capacitance "C'" has been replaced by the normalized resistance "R'". Therefore, the amplifier gain "K" will be designated as the variable alpha, and the normalized resistance "R'" will replace the normalized capacitance "C'" as the variable beta.

3.8. Figures 3-11 and 3-12 are examples of the frequency response for this network configuration. If these families of curves were to be rotated about the omega = 1 axis, it is seen that they are indeed similar to the curves obtained for the previous configuration when the load impedance was the capacitance "C_z". Examining these curves, note that the area between omega = 1.05 and omega = 1.6 again resembles the frequency response expected from a second order system with a pair of complex conjugate poles.

From figure 3-11 it appears that the stability limit is achieved for a value of amplifier gain 'K' equal to 3.0. By substituting into equation 3-8, it is found that

$$K \leq 3.0$$

which agrees with the value determined graphically. Utilizing this information, a desired frequency response can again be selected. For the remainder of this illustration, the frequency response associated with

amplifier gain 'K' = 2.0

component ratio'k' = 2.0

normalized resistance "R'" = 0.5

will be utilized.

3.9. Figures 3-13 through 3-18 are the constant bandwidth curves to be utilized with figure 3-11. Again the network component ratio 'k' has been maintained at a constant value, in this case 2.0, and each graph represents a different value of omega. For this configuration, the normalized

resistance "R'" now becomes the abcissa variable while the ordinate variable, amplifier gain 'K' and the 2 db separation between curves remain the same as for the first configuration. In figure 3-11, the magnitude between successive curves has the greatest variation in the area omega = 1.05 to omega = 1.60. Utilizing the same criterion as before, that of remaining within plus or minus 1db, acceptable tolerances can be determined for the amplifier gain "K" and the normalized resistance "R'". From figure 3-17 it is seen that point A, the position of the selected operating values, is located where the constant 2.5db curve would appear. Thus utilizing the plus or minus 1db deviation criteria, the amplifier gain "K" can vary over the range of 1.92 to 2.08. A similar examination of the remaining constant bandwidth curves results in the following values:

omega = 0.8	$1.87 < K < 2.13$
omega = 1.1	$1.88 < K < 2.12$
omega = 1.2	$1.90 < K < 2.10$
omega = 1.4	$1.92 < K < 2.08$
omega = 1.8	$1.90 < K < 2.08$

It can be seen that the differences between the operating ranges of the amplifier gain for the various omega values does not change appreciably when compared to the differences observed for the previous example. This is due to the fact that the selected operating values have resulted in the system being further displaced from the area of instability.

In determining the tolerance range of the normalized resistance "R'", figures 3-16 and 3-17 will be utilized. From both figures it is seen that the normalized resistance "R'" can vary over the range 0.46 to 0.54 when the amplifier gain "K" is equal to 2.0.

To determine the allowable tolerances of the amplifier gain "K" and the normalized resistance "R'" as a combination and remain within the plus or minus 1db specification, either figure 3-16 or 3-17 can be used. When the amplifier gain "K" is restricted to the range $1.94 \leq K \leq 2.06$, a tolerance of plus or minus 3 percent, the normalized resistance "R'" can vary over the interval 0.47 to 0.53 which is a tolerance of plus or minus 6 percent.

3.10. With the determination having been made that the selected operating values are acceptable, the remaining values of the network elements can be determined after selecting the desired notch frequency. Utilizing the 1.59 KHz selected for the previous example and a capacitance value of 0.01μ farads from equation 3-2, the resistance "R" is again equal to 10 K ohms. With the component ratio "k" now equal to 2.0 and the normalized resistance "R'" equal to 0.50, the remaining element values are:

$C/k = 0.005\mu$ farads

$(k+1/k)C = 0.015\mu$ farads

$kR = 20$ K ohms

$$(k/k+1)R = 6.67 \text{ K ohms}$$

$$R_Z = R/R' = 20 \text{ K ohms}$$

Inserting the computed values into figure 3-1 results in the completed circuit of figure 3-1b.

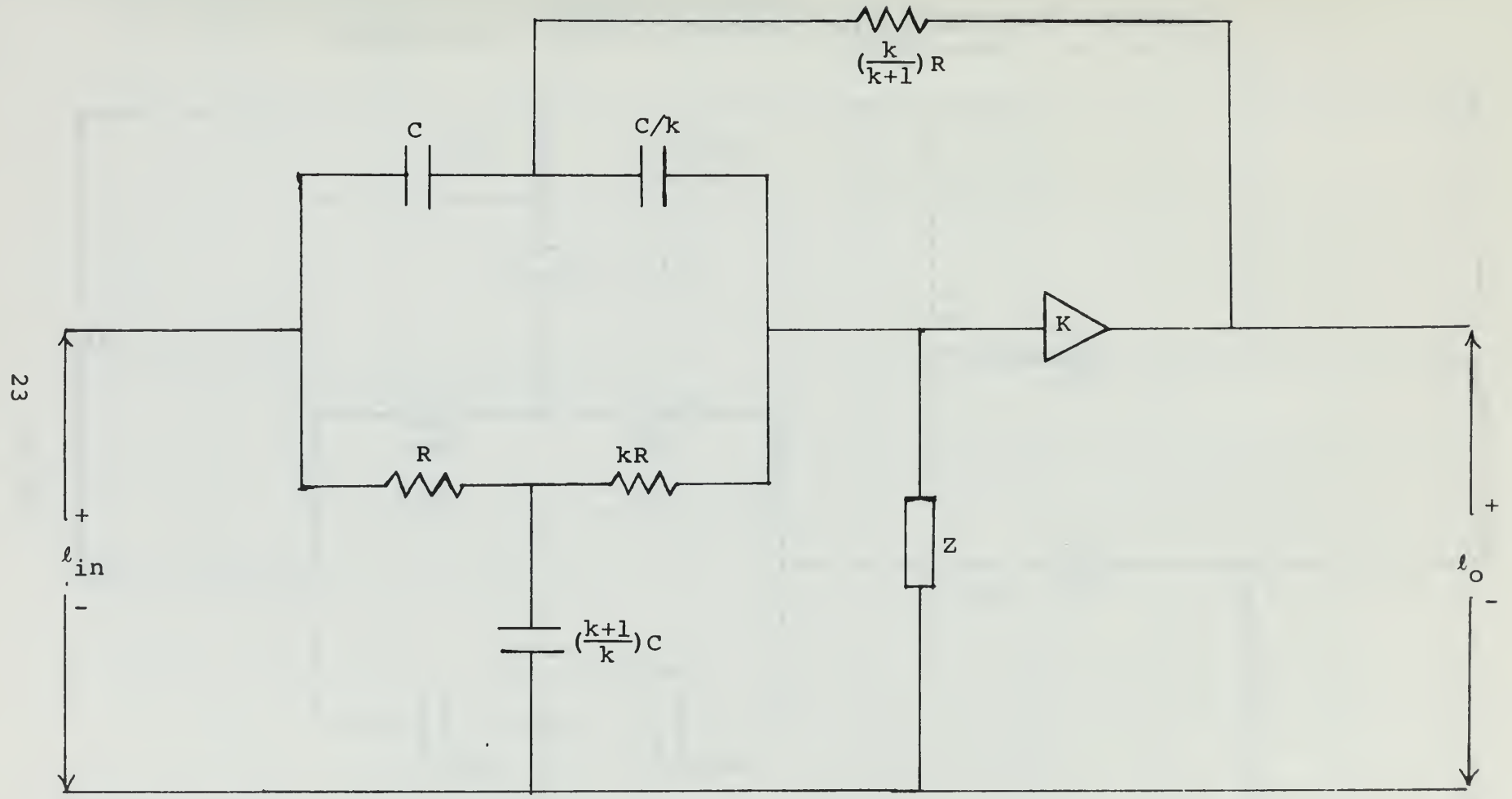

Figure 3-1. Circuit Diagram, Active Parallel-T Network

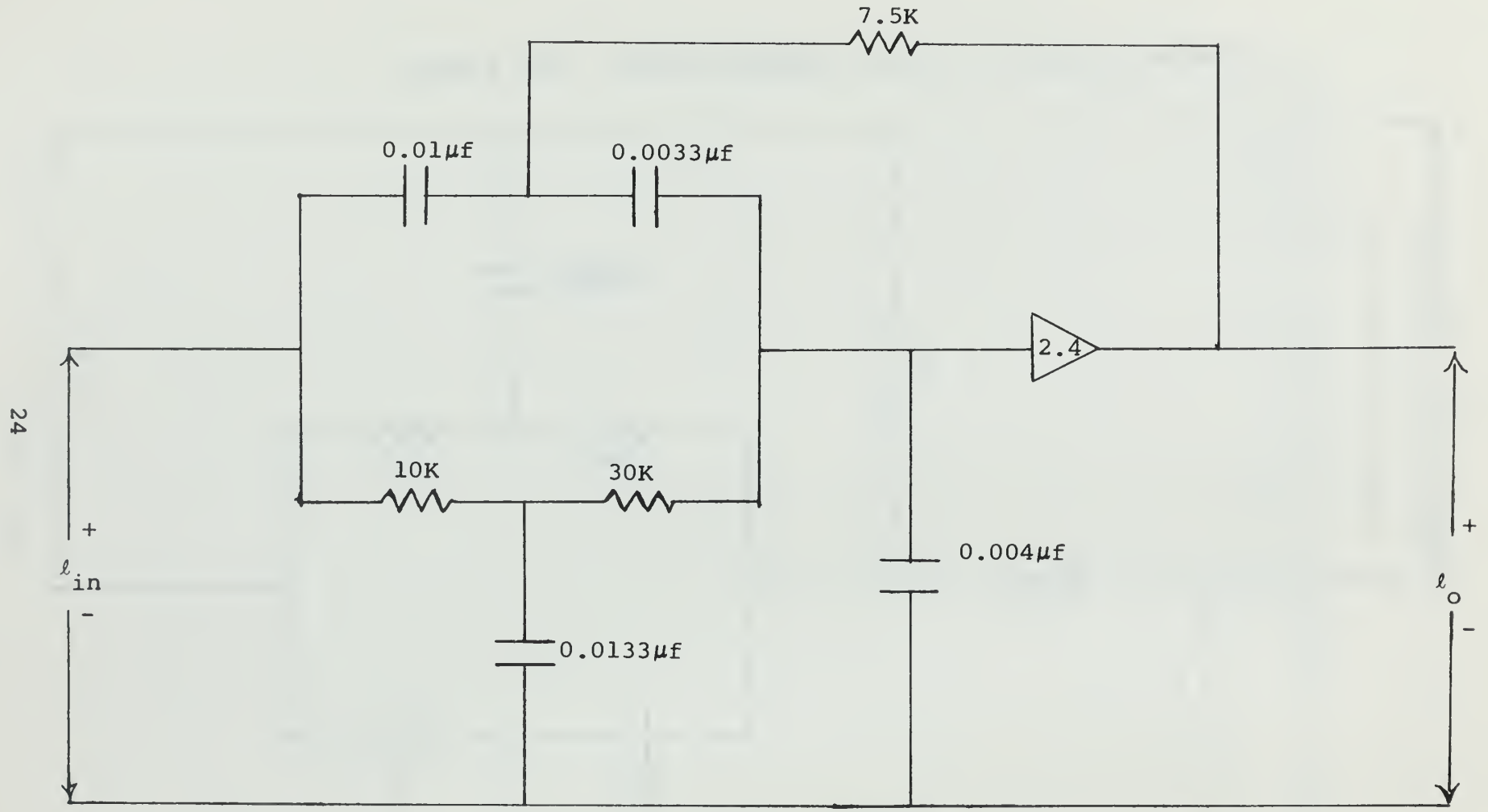

Figure 3-1a. Circuit Diagram, Active Parallel-T Network
Capacitive Load

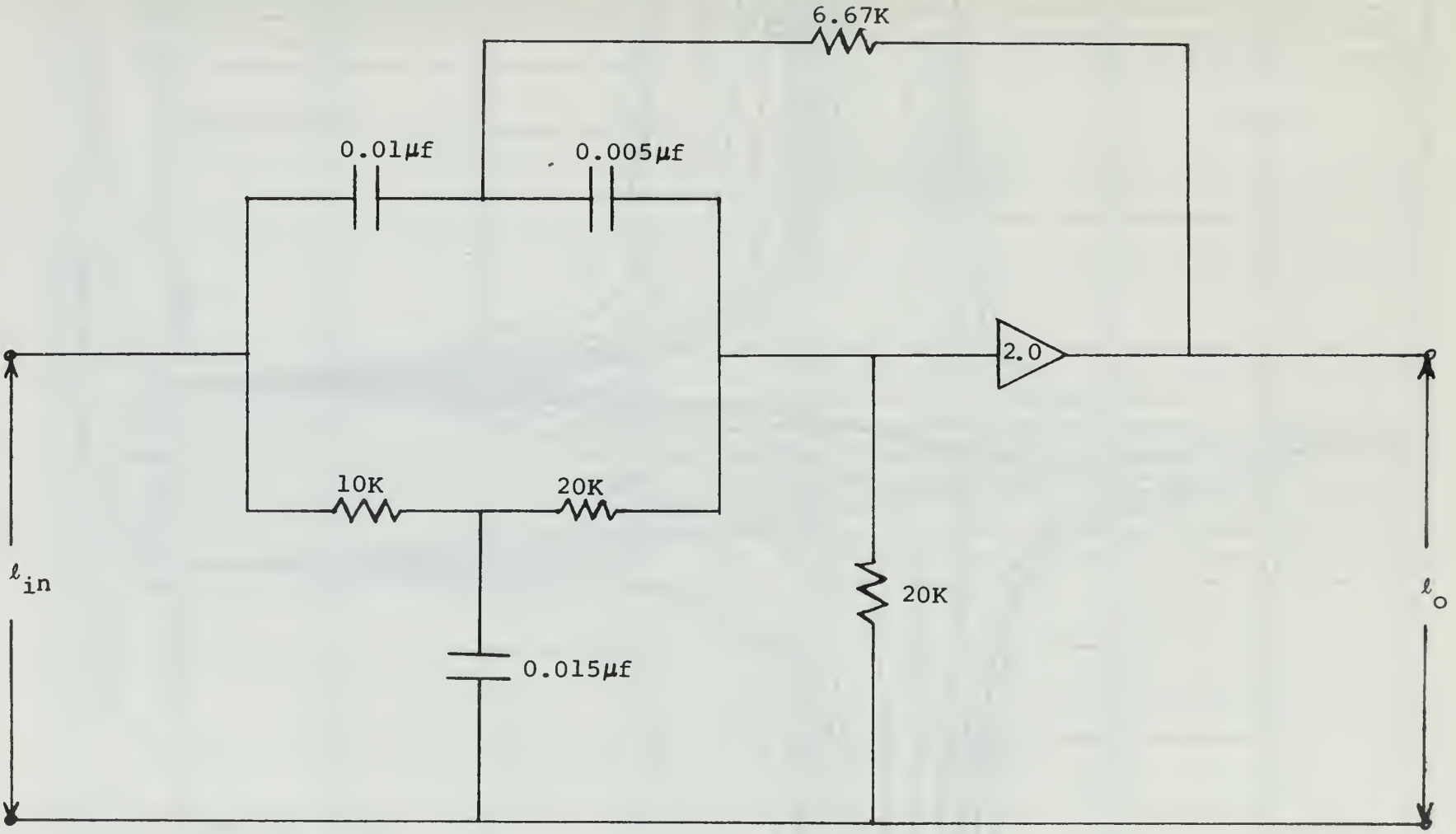

Figure 3-1b. Circuit Diagram, Active Parallel-T Network, Resistive Load

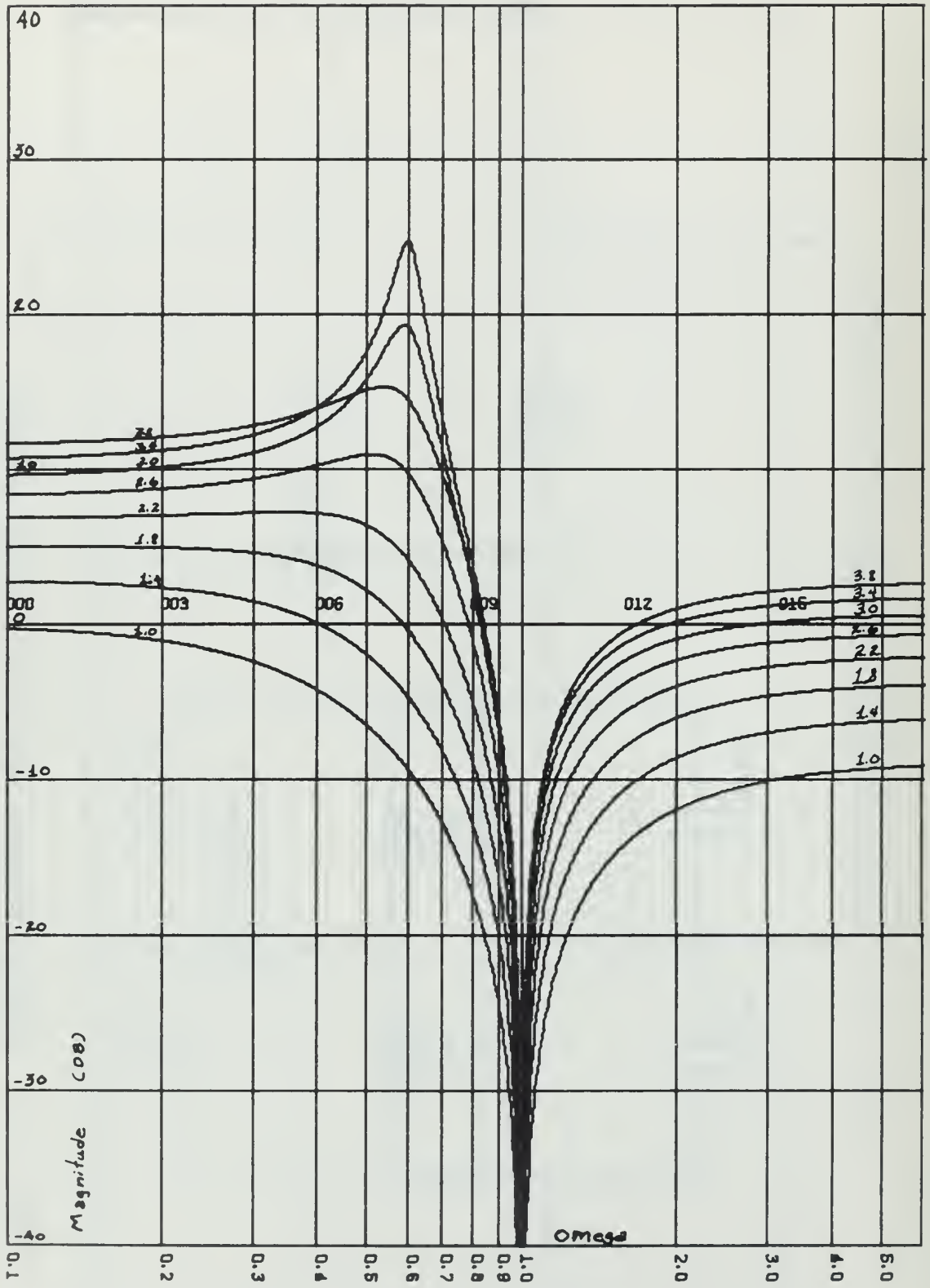

Figure 3-2. Frequency Response of the Active Parallel-T Network with a Capacitive Load. k=2.5, C'=0.5

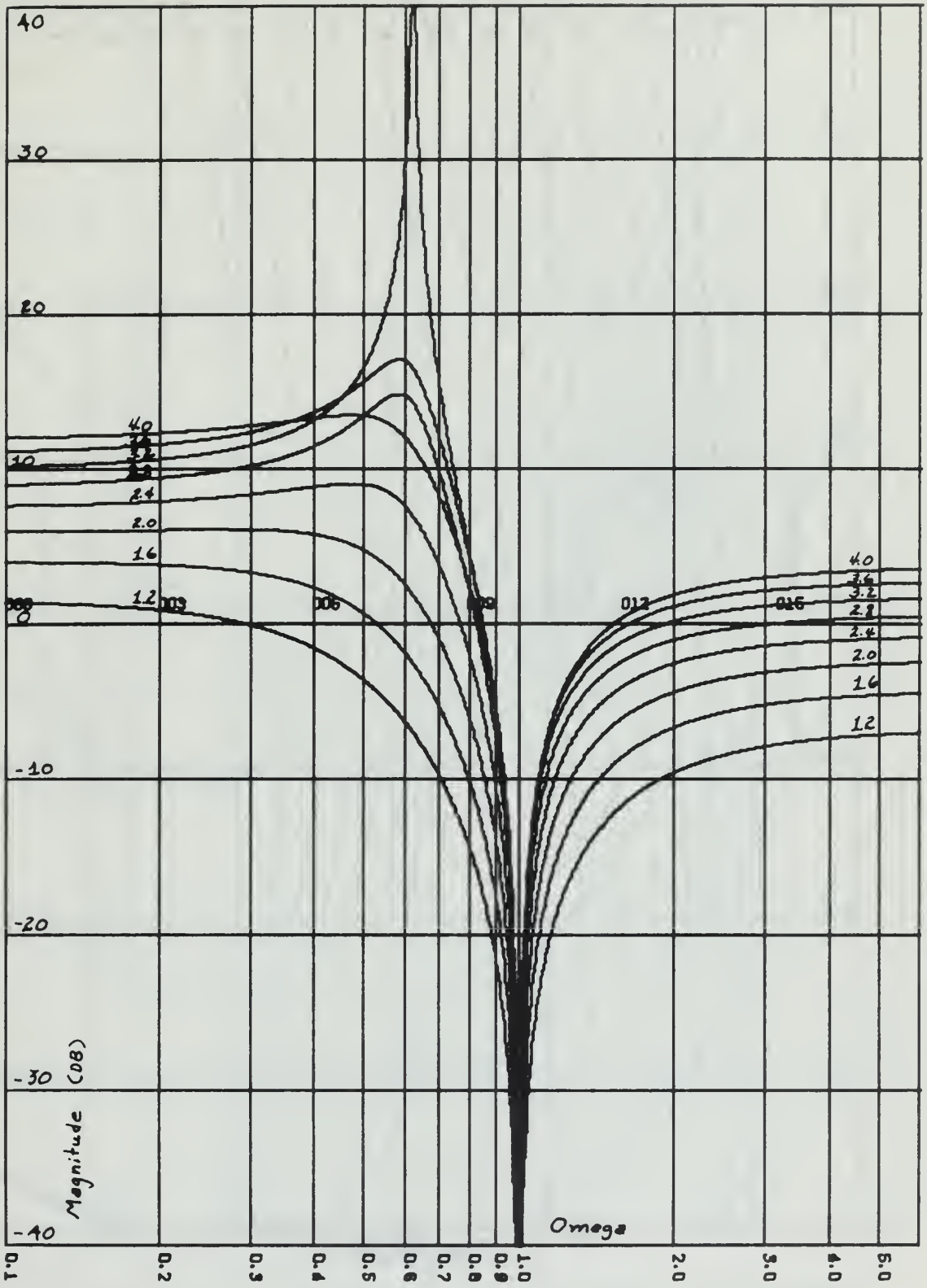

Figure 3-3. Frequency Response of the Active Parallel-T Network with a Capacitive Load. k=3.0, C'=0.4

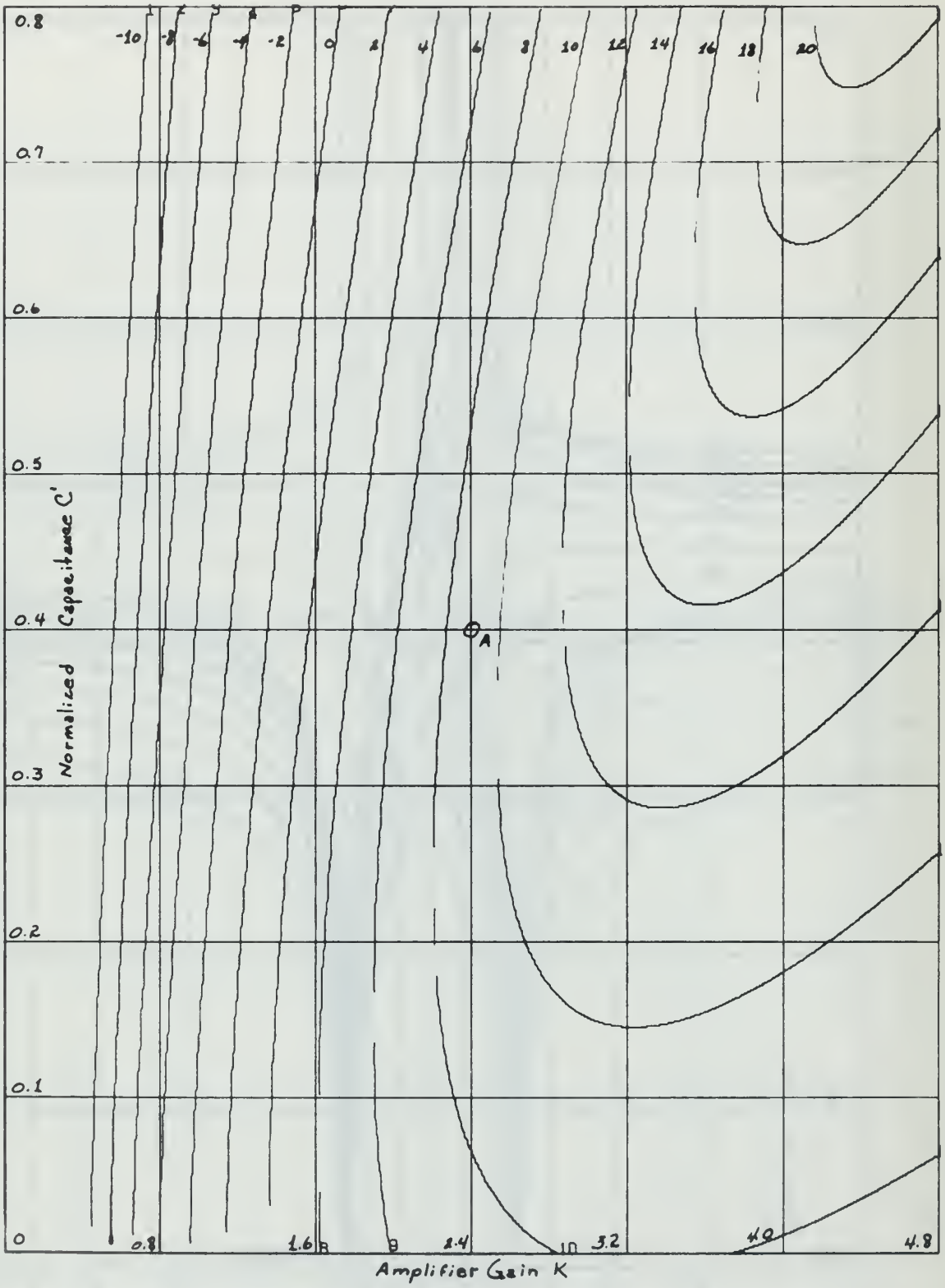

Figure 3-4. Constant Bandwidth Curves of the Active Parallel-T Network at Omega = 0.4 for a Capacitive Load

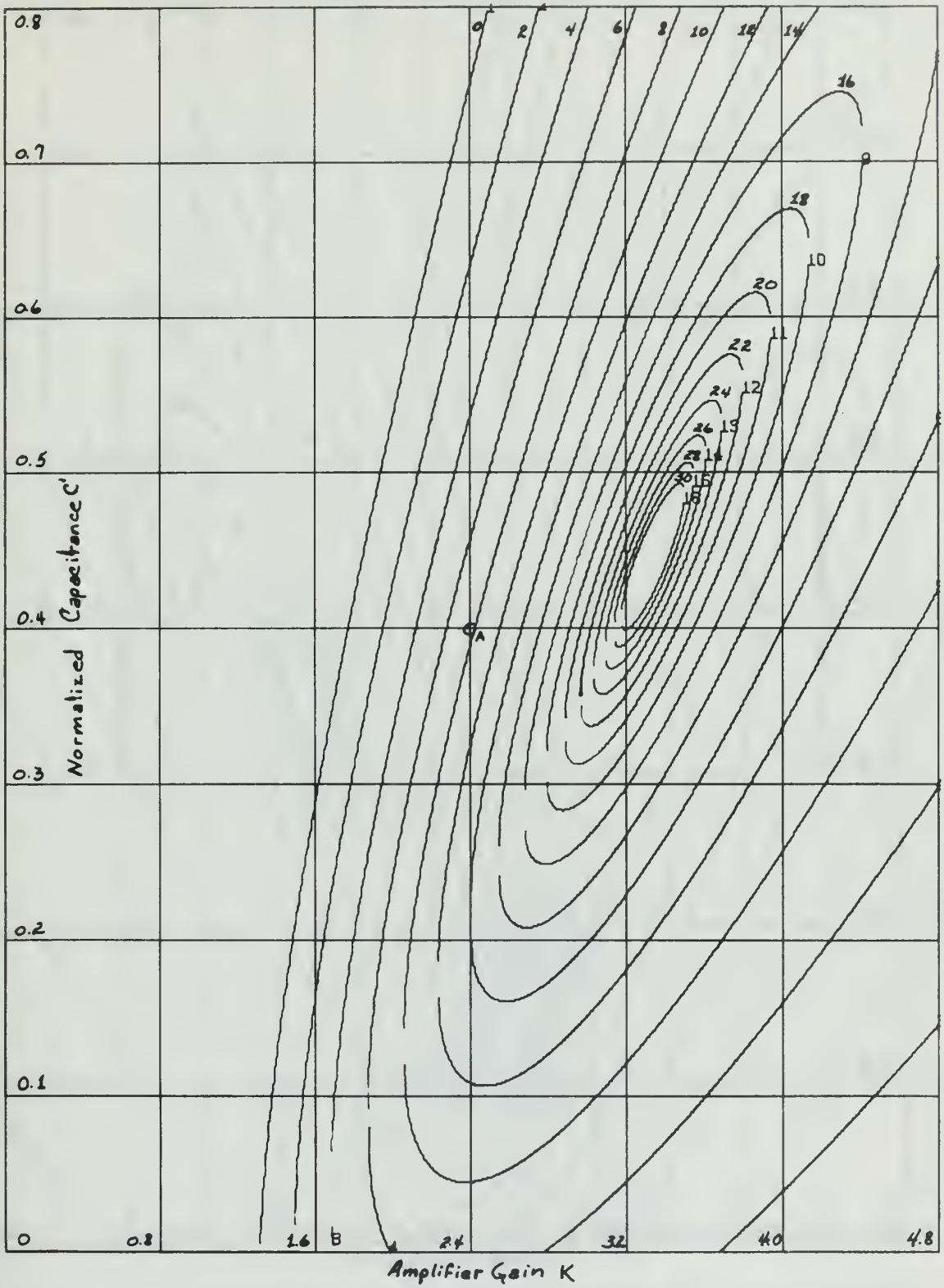

Figure 3-5. Constant Bandwidth Curves of the Active Parallel-T Network at Omega = 0.6 for a Capacitive Load

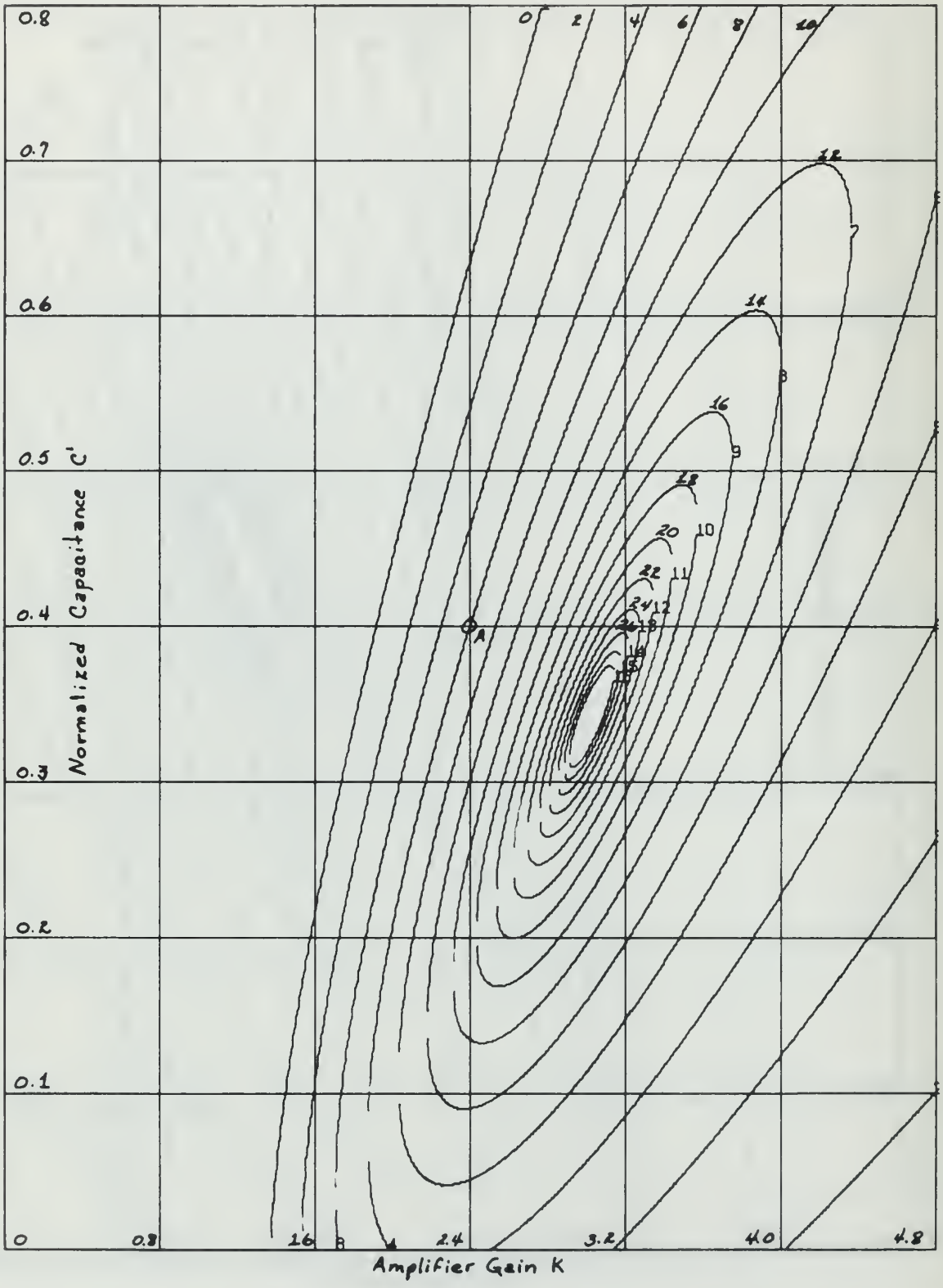

Figure 3-6. Constant Bandwidth Curves of the Active Parallel-T Network at Omega = 0.65 for a Capacitive Load

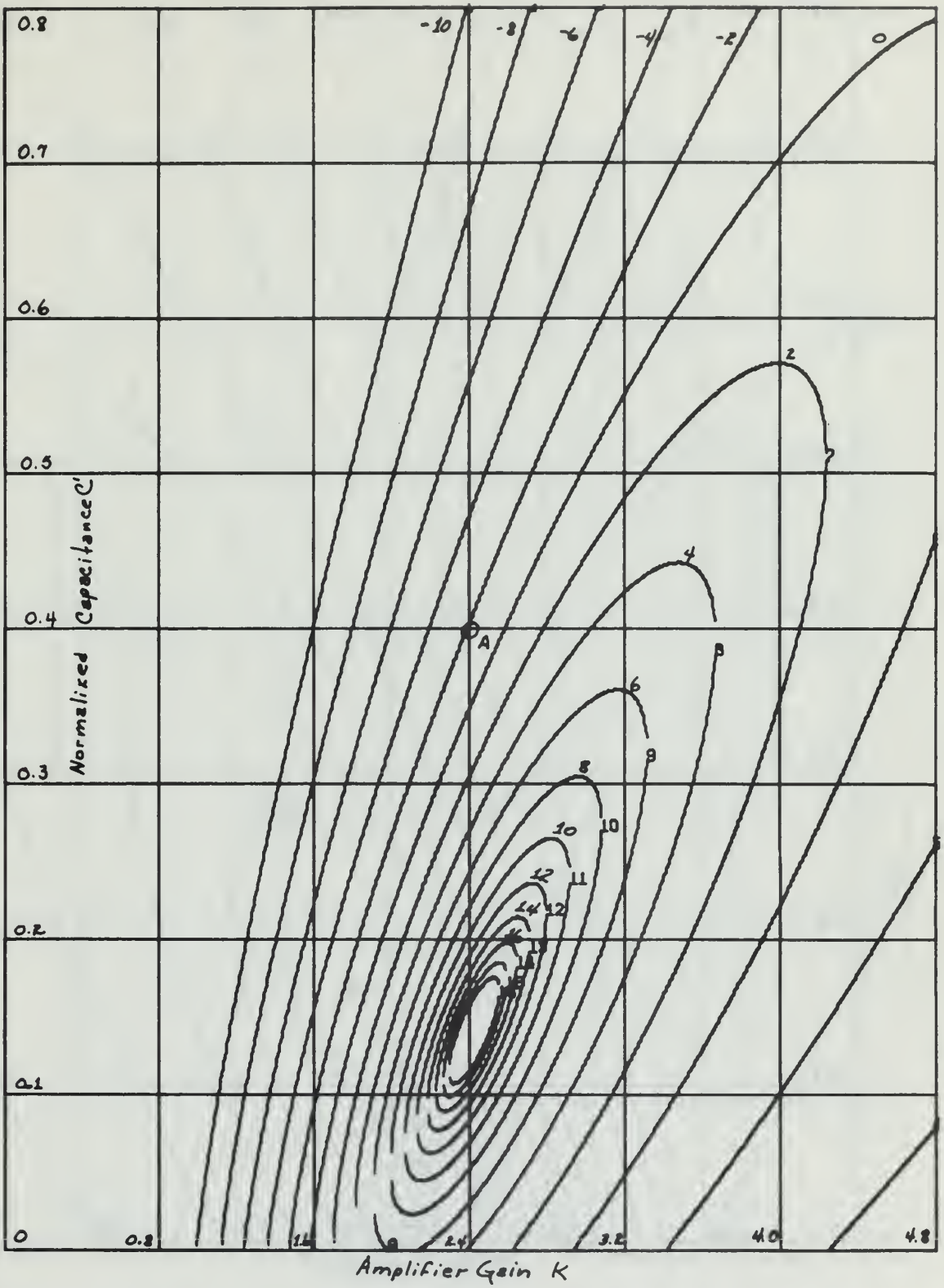

Figure 3-7. Constant Bandwidth Curves of the Active Parallel-T Network at Omega = 0.8 for a Capacitive Load

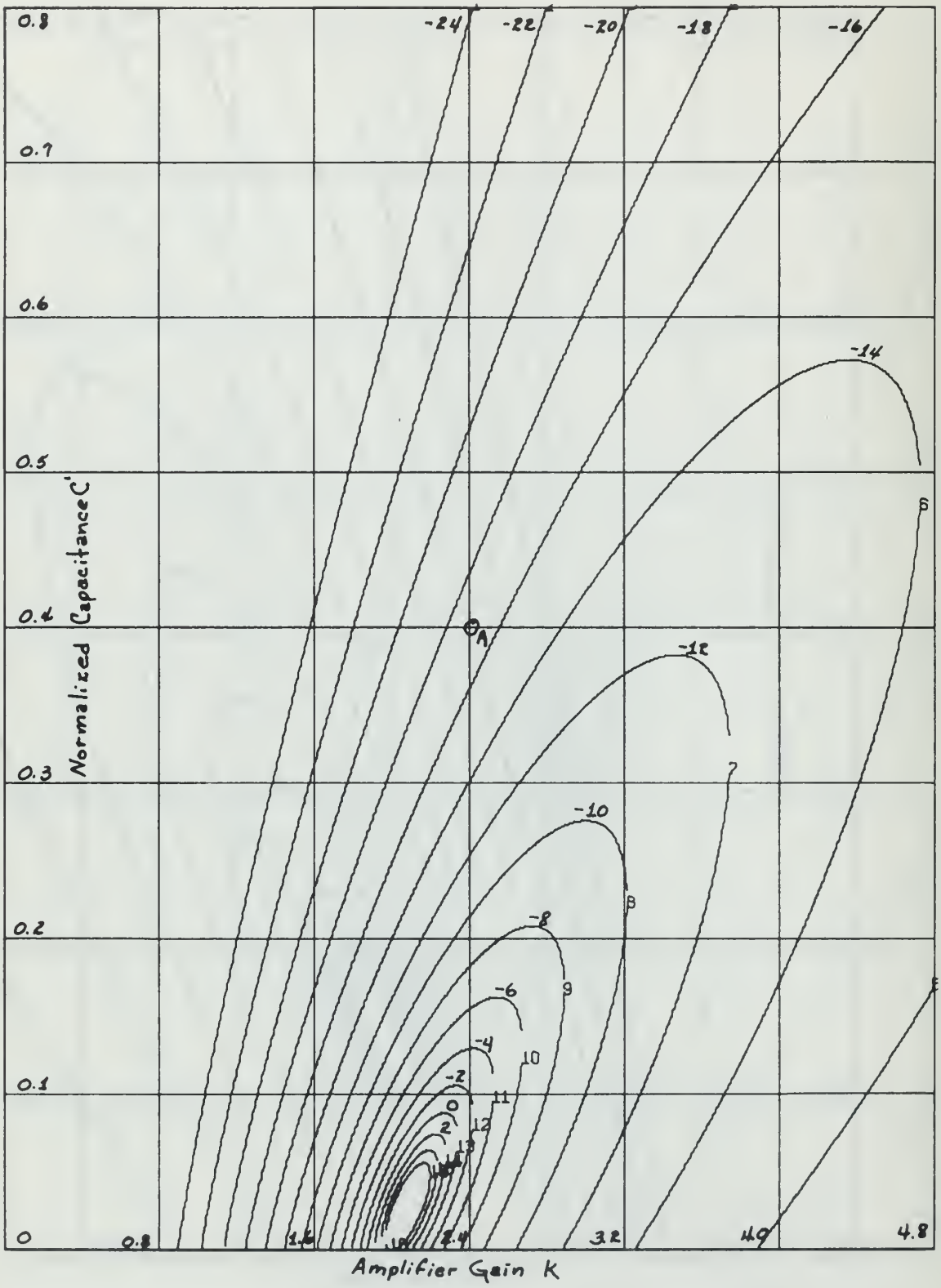

Figure 3-8. Constant Bandwidth Curves of the Active Parallel-T Network at Omega = 0.95 for a Capacitive Load

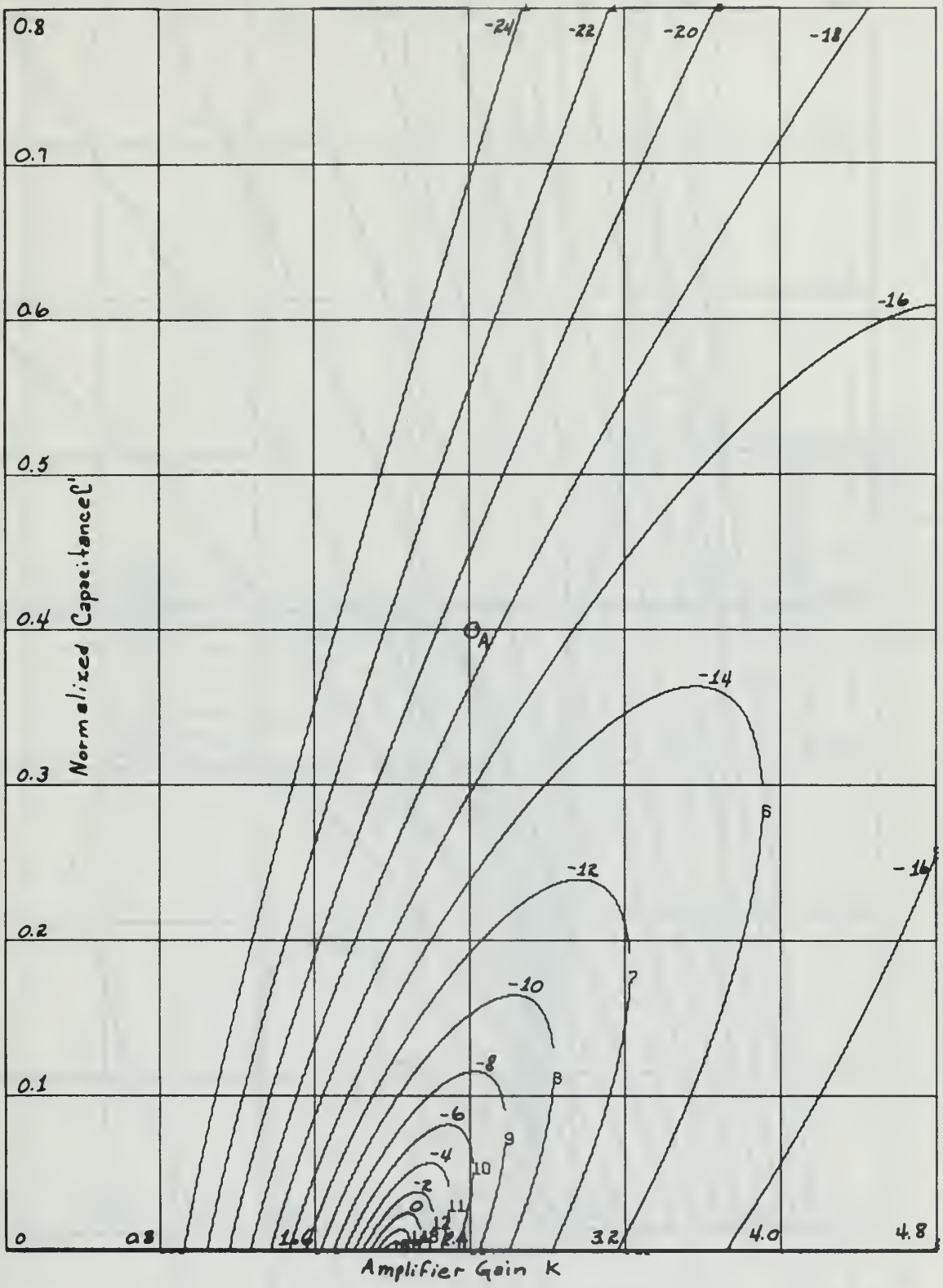

Figure 3-9. Constant Bandwidth Curves of the Active Parallel-T Network at Omega = 1.05 for a Capacitive Load

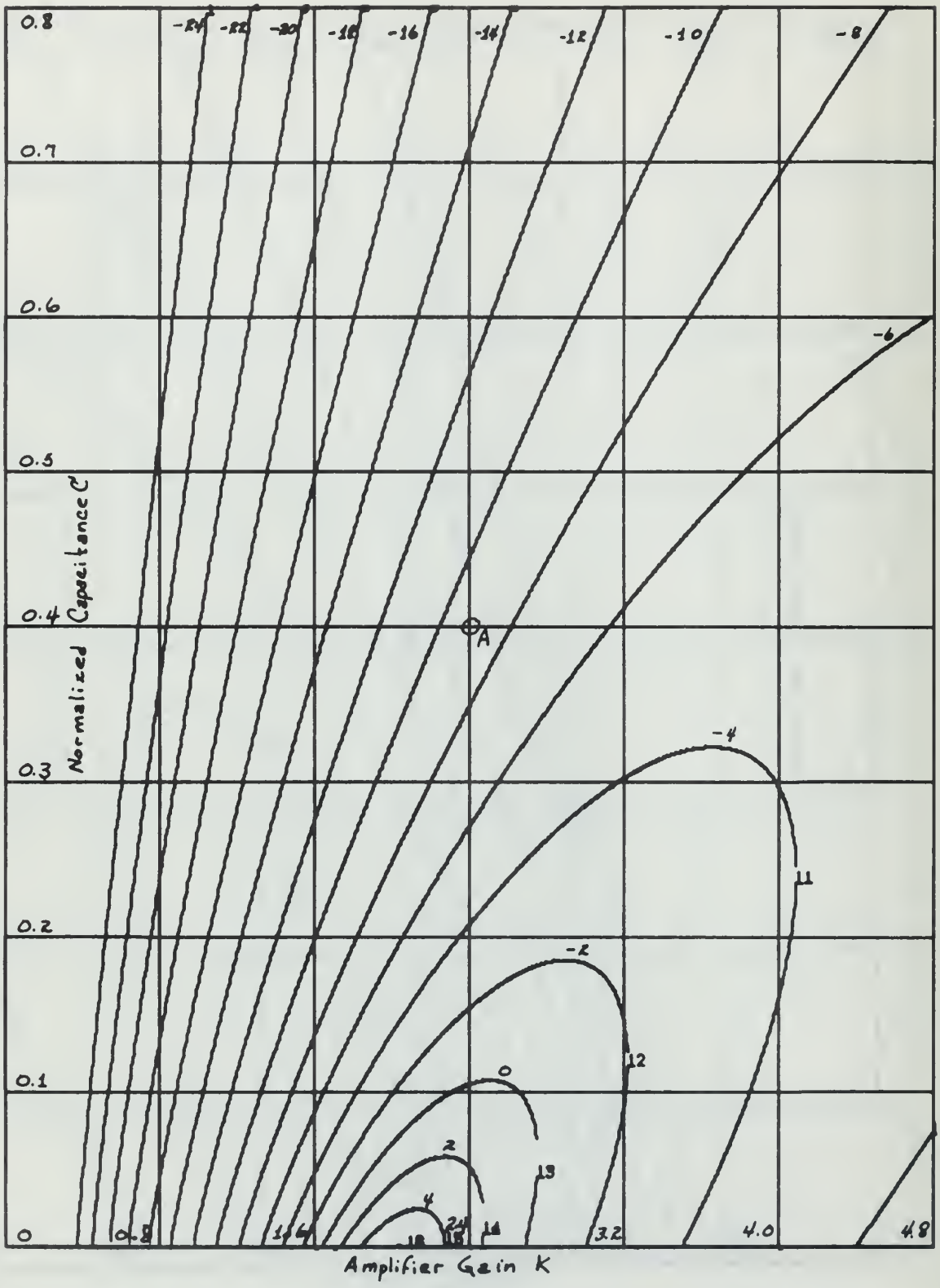

Figure 3-10. Constant Bandwidth Curves of the Active Parallel-T Network at Omega = 1.2 for a Capacitive Load

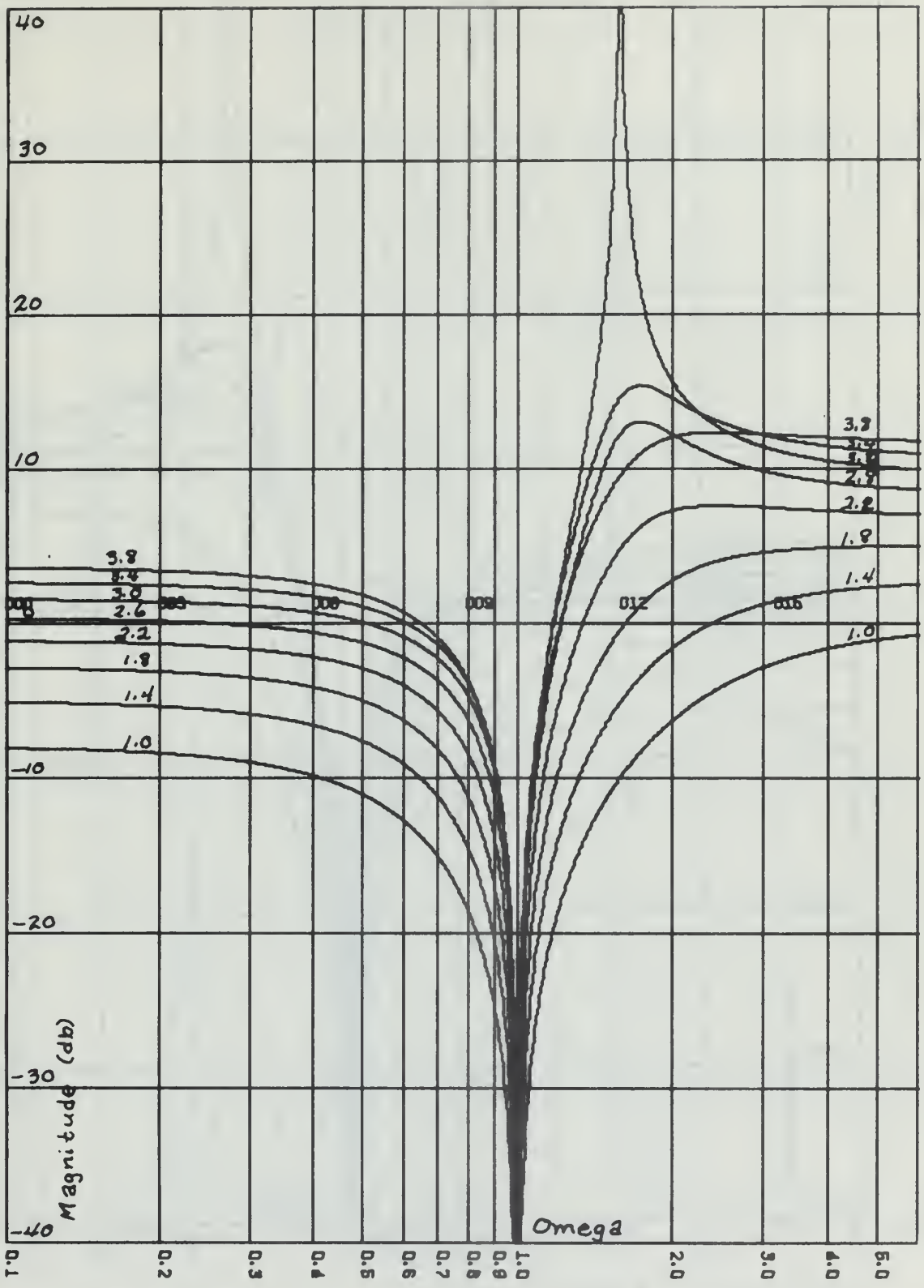

Figure 3-11. Frequency Response of the Active Parallel-T Network with a Resistive Load. k=2, R'=0.5

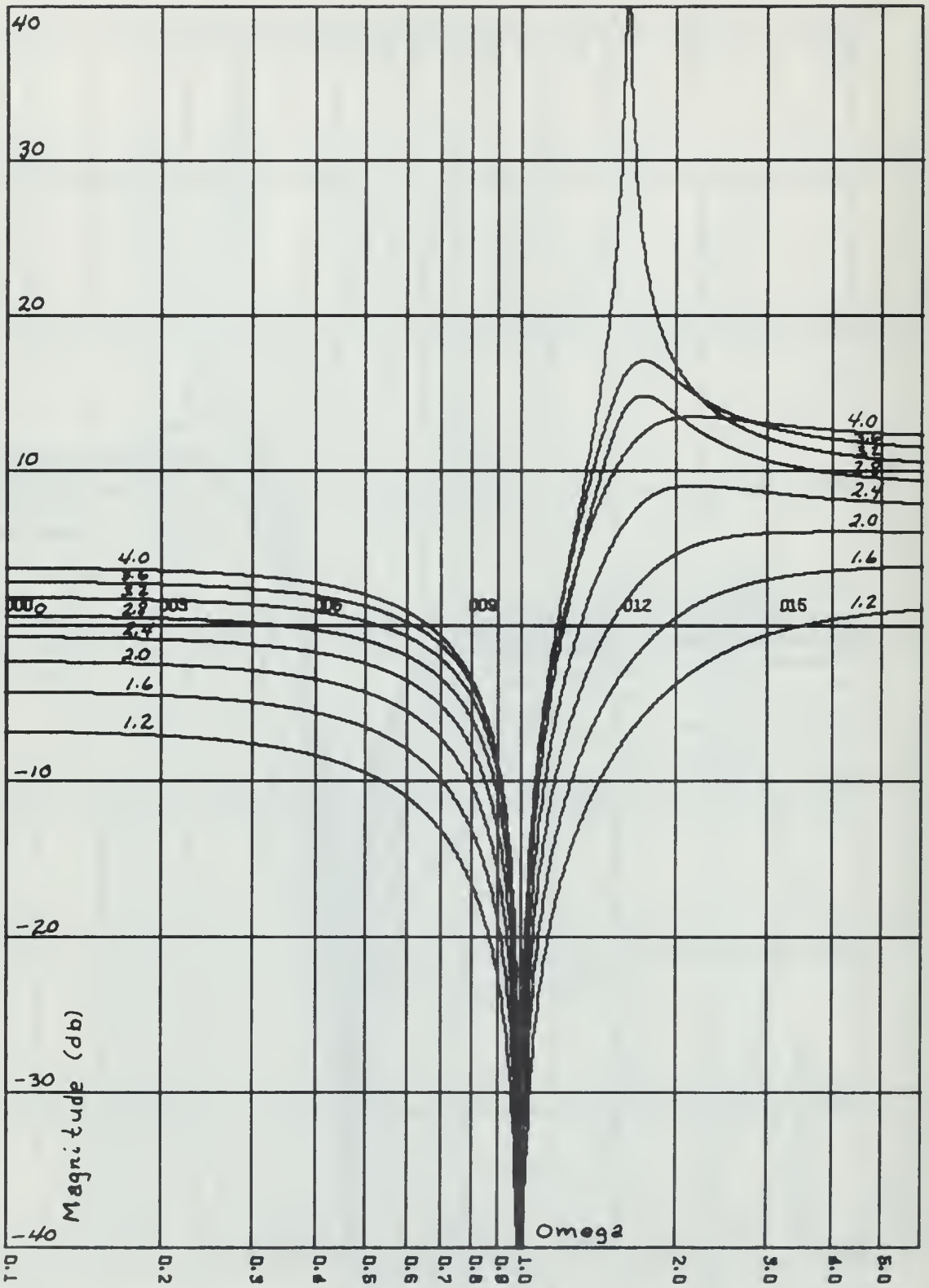

Figure 3-12. Frequency Response of the Active Parallel-T Network with a Resistive Load. k=3.0, R'=0.4

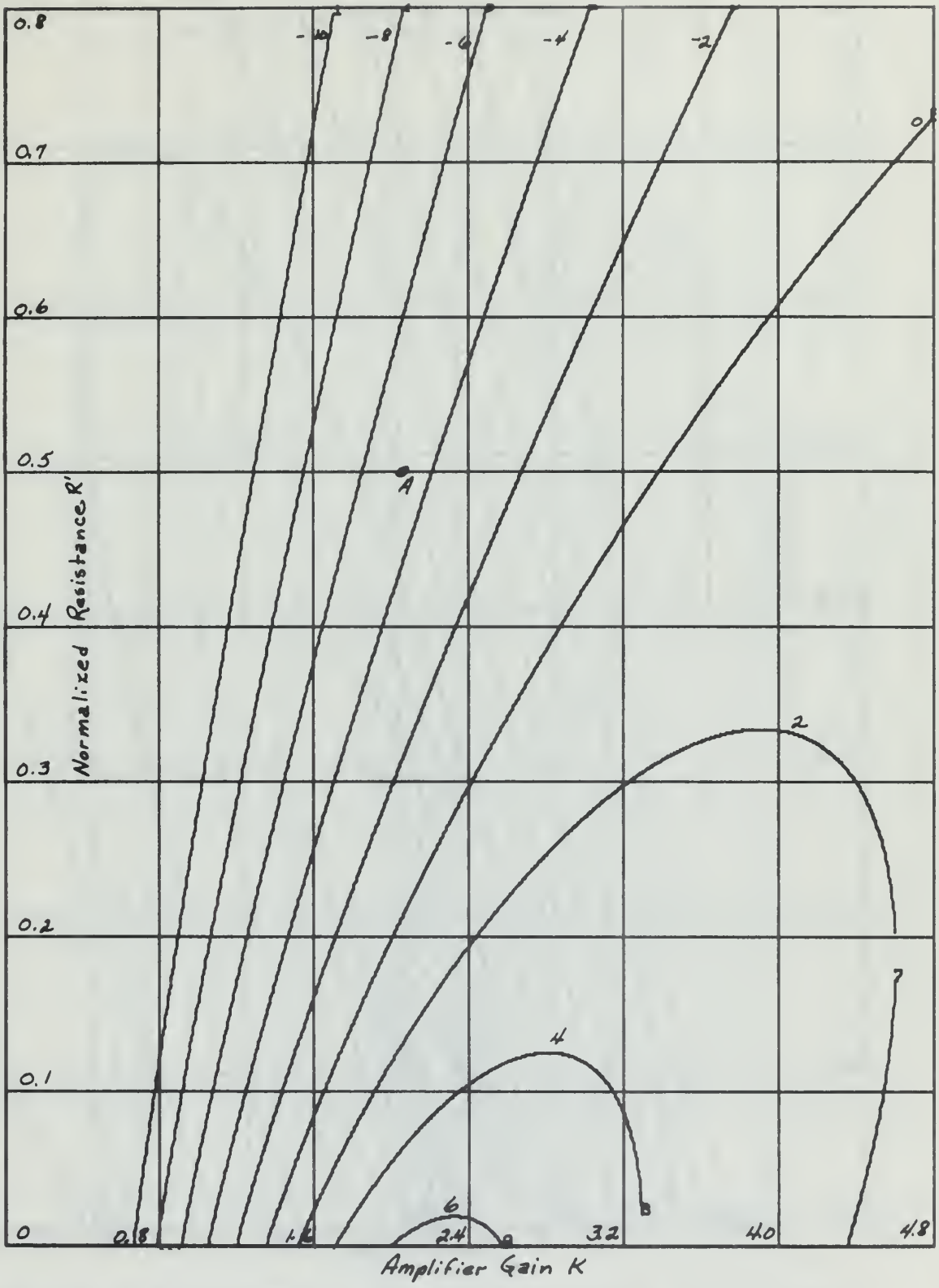

Figure 3-13. Constant Bandwidth Curves of the Active Parallel-T Network at Omega = 0.8 for a Resistive Load

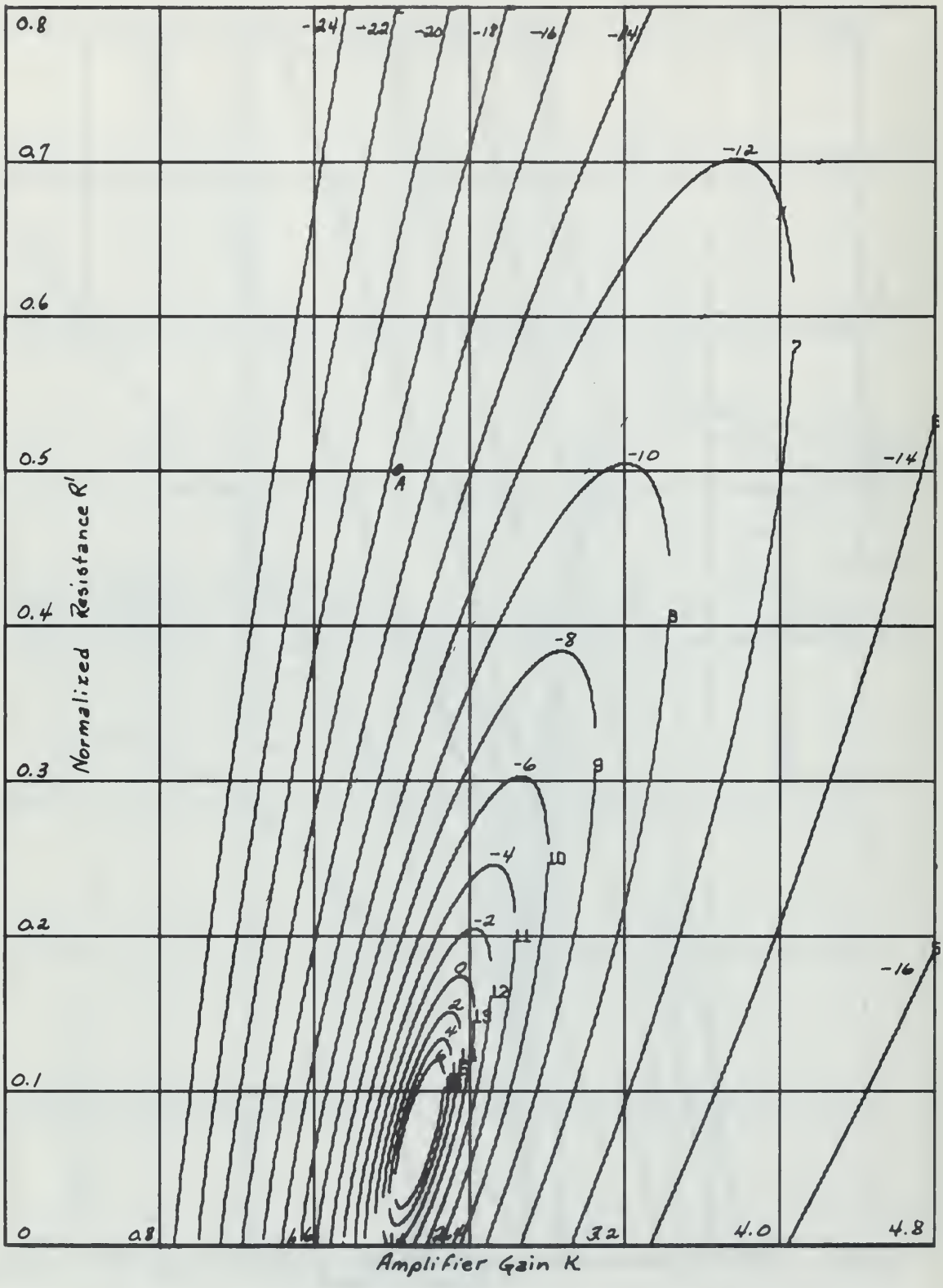

Figure 3-14. Constant Bandwidth Curves of the Active Parallel-T Network at Omega = 1.1 for a Resistive Load

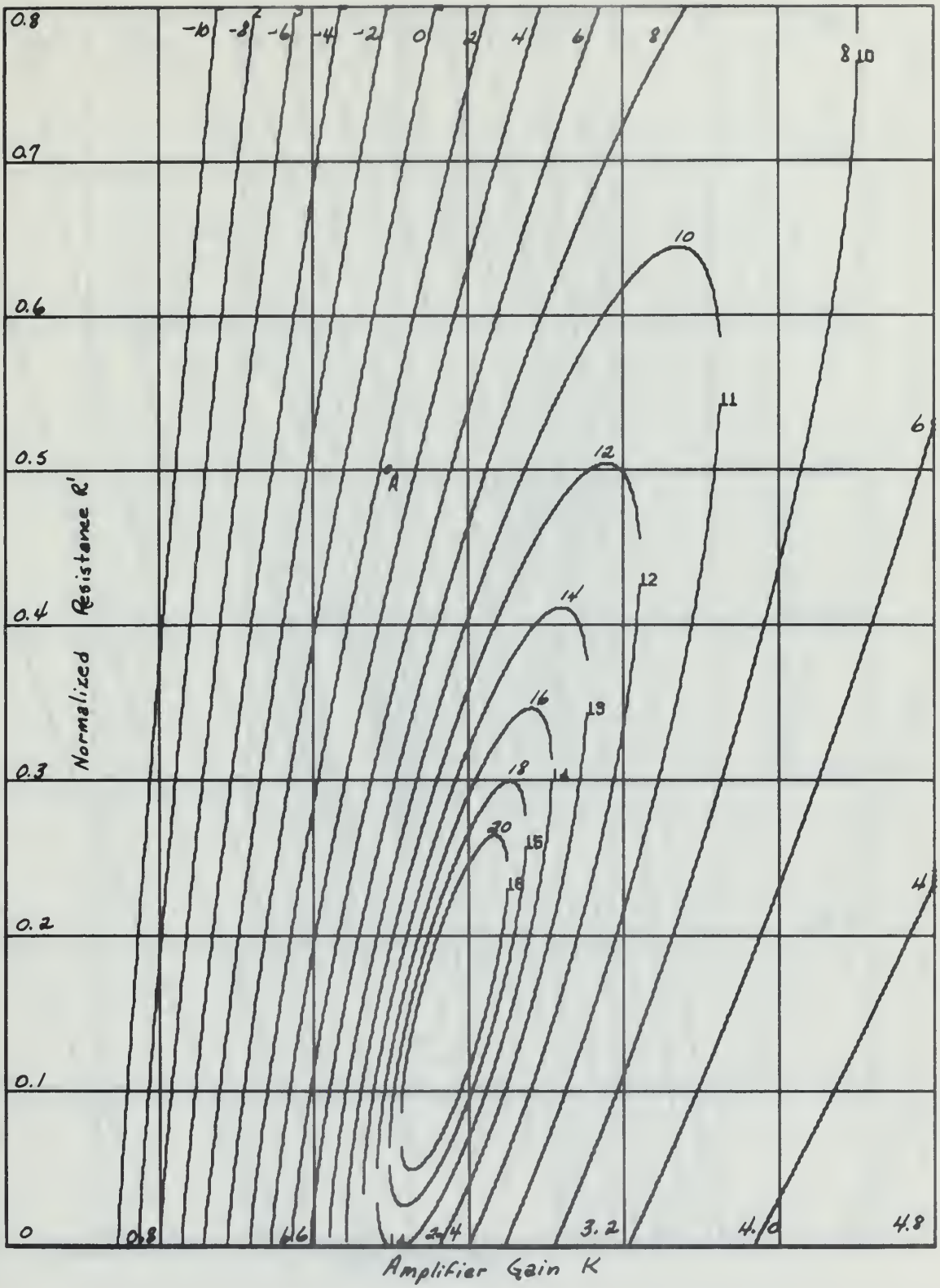

Figure 3-15. Constant Bandwidth Curves of the Active Parallel-T Network at Omega = 1.2 for a Resistive Load

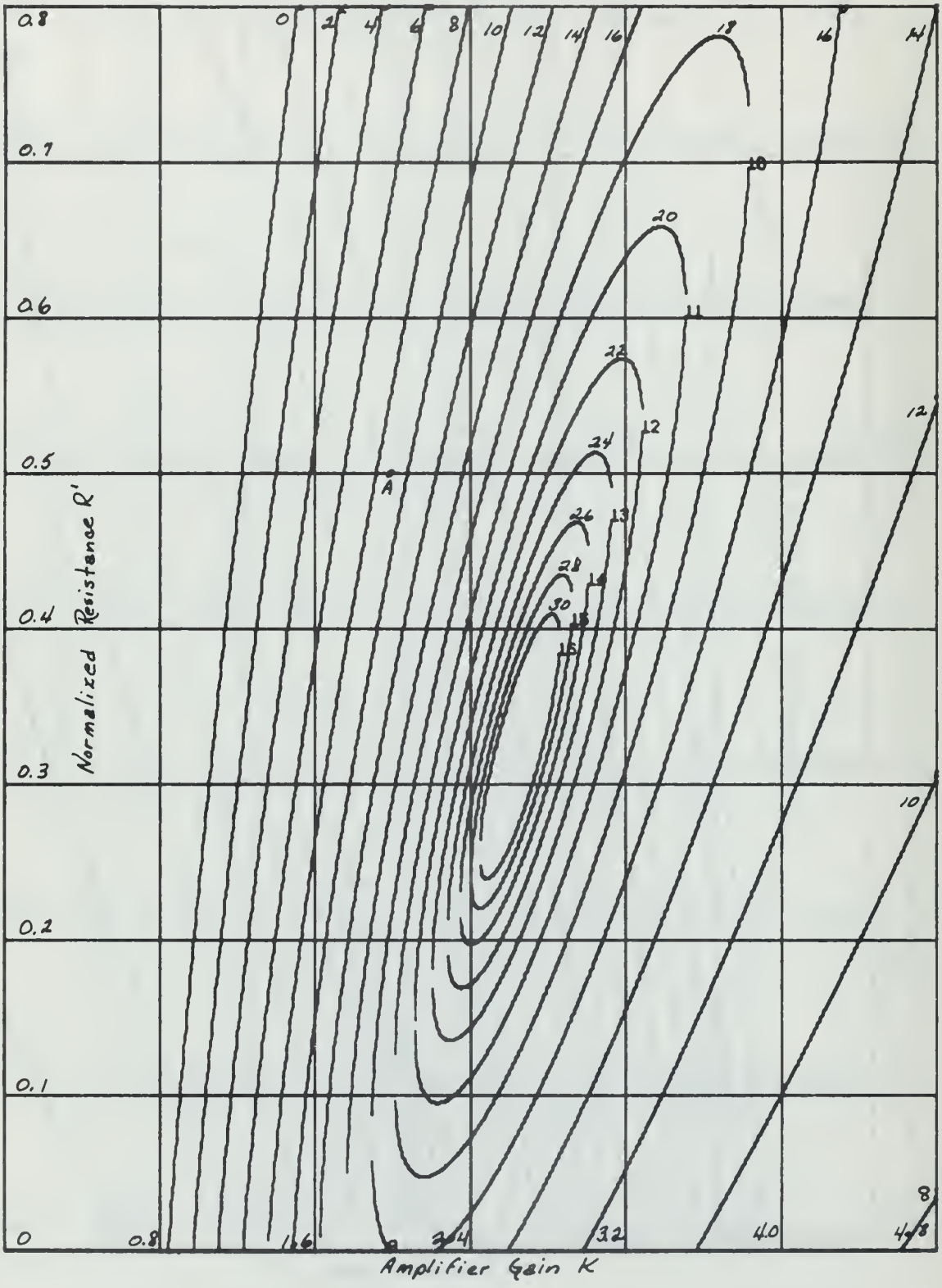

Figure 3-16. Constant Bandwidth Curves of the Active Parallel-T Network at Omega = 1.4 for a Resistive Load

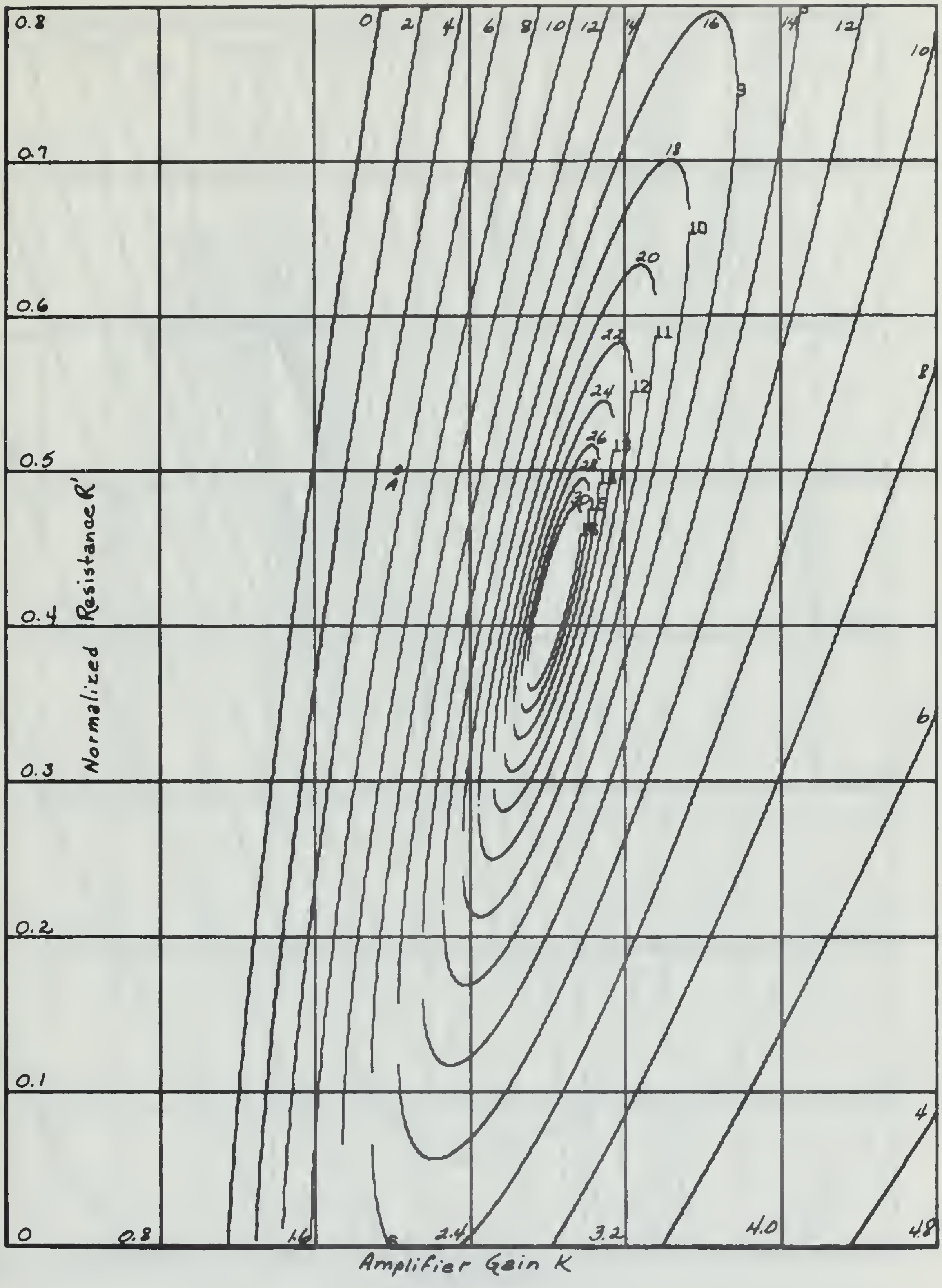

Figure 3-17. Constant Bandwidth Curves of the Active Parallel-T Network at Omega = 1.5 for a Resistive Load

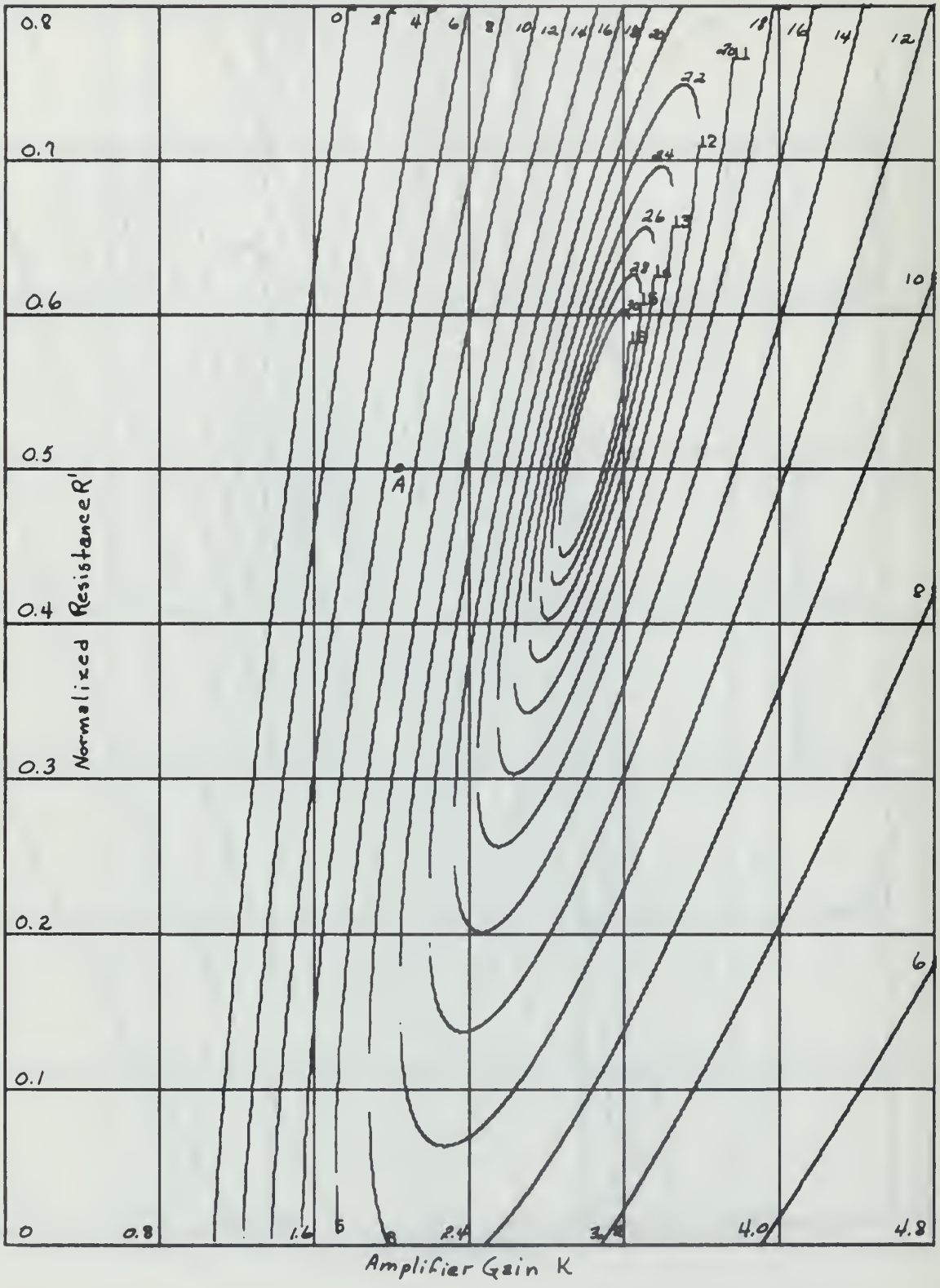

Figure 3-18. Constant Bandwidth Curves of the Active Parallel-T Network at Omega = 1.6 for a Resistive Load

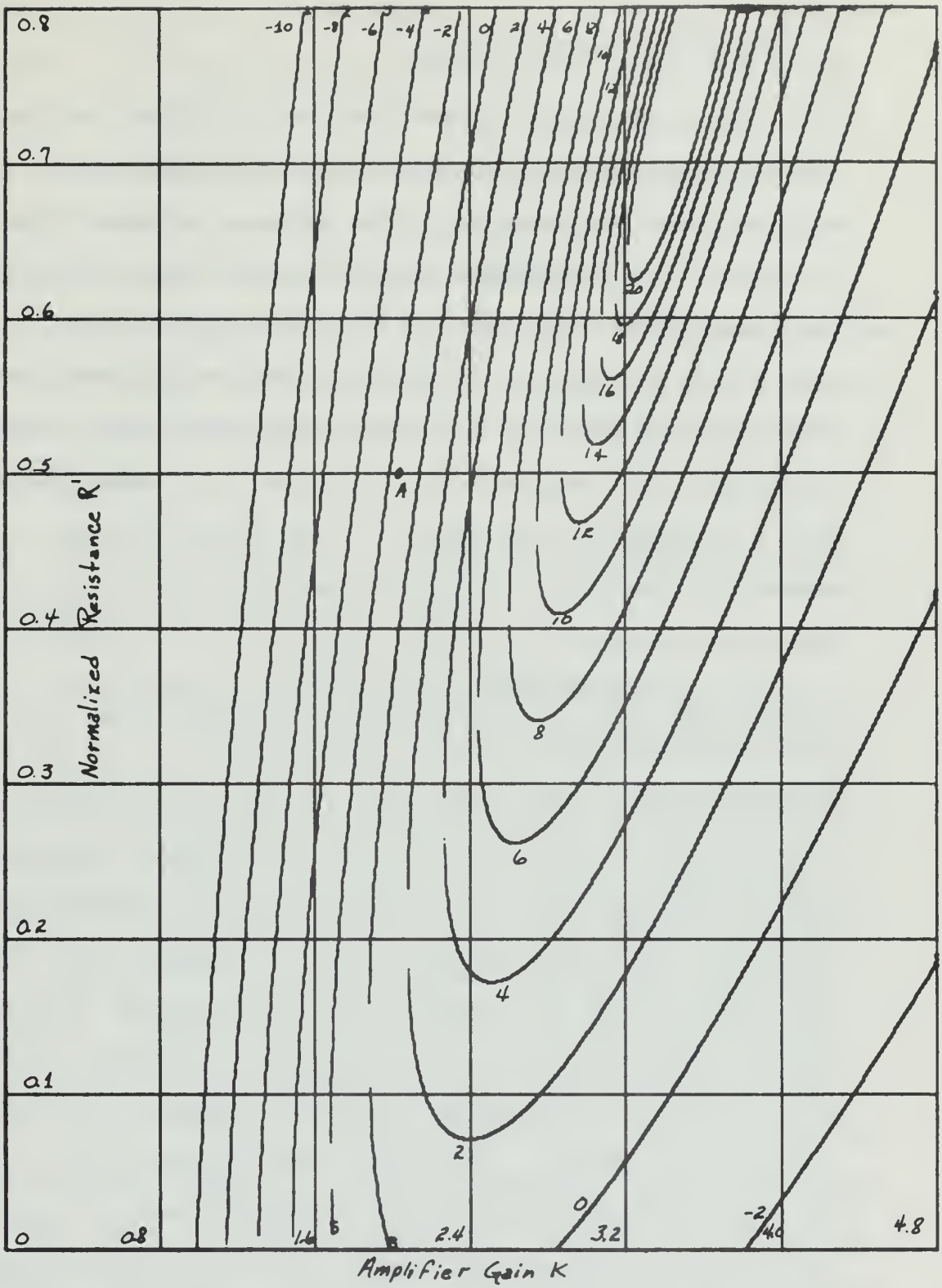

Figure 3-19. Constant Bandwidth Curves of the Active Parallel-T Network at Omega = 1.8 for a Resistive Load

4. THE DOUBLE TUNED FILTER

4.1. To investigate the utilization of parameter planes in the design of higher order systems, the double tuned filter of figure 4-1 was examined. The purpose of this filter is to provide two separately tuned networks which results in a very high Q for the system. An example of the high Q of this filter is shown in figure 4-2 where the amount of attenuation in db has been plotted versus frequency. It can be noted that the response of the system has changed by 40 db over a frequency range which is less than an octave. By examining figure 4-1, it can be seen that there are six capacitors present which will result in the transfer function of the system having a sixth order denominator. However, by considering the two amplifiers as being operational amplifiers so that the output voltage of the amplifier is equal to the input voltage to the amplifier times the gain of the amplifier, the network can be separated into the three individual sections shown in figure 4-3. With this stipulation, the overall transfer function of the double tuned filter can be determined by finding the transfer functions of the three individual sections and multiplying them together. The individual sections are first, second and third order systems which will result in transfer functions having polynomials which are easier to examine. By examining the three individually we see that the circuit has essentially been separated into an active low

pass filter, an active bandpass filter and a RC high pass filter. In designing the double tuned filter, the three sections will first be considered separately to determine the individual responses, then various combinations will be investigated to determine if the actual results agree with the results that would be expected.

The transfer functions of the three individual systems have been derived and are available in Appendix A. In this section only the final results of these derivations will be specified.

4.2. From equation (3) of Appendix A the transfer function of section 1 of figure 4-3 is

$$T_1(s) = \frac{(A/R_1C_1)\left(s + (1/R_2C_2)\right)}{s^2 + s\left(R_1C_1+R_2C_2+(1-A)R_1C_2\right)/R_1C_1R_2C_2+(1/R_1C_1R_2C_2)} \qquad (4\text{-}1)$$

Since the purpose of the entire network is to act as a high Q bandpass filter, two possibilities exist concerning the poles of this transfer function. One is to have two real poles both located to the right of the zero on the Bode diagram. Under this configuration, the db rise and drop would be 20 db per decade. The second possibility is to have a pair of complex conjugate roots as the two poles of the transfer function. When the damping coefficient, zeta, is very small, a very distinct peak can be obtained at the desired frequency. This peak will have a db rise and fall which will be considerably greater than the 20 db per

decade encountered under the first possibility. Since a high Q network is desired, the second possibility will be examined.

From equation 4-1,

$$\omega_n = 1/\sqrt{R_1C_1R_2C_2} \tag{4-2}$$

and

$$2\zeta\omega_n = \frac{1}{R_1C_1R_2C_2}\left(R_1C_1+R_2C_2+(1-A)R_1C_2\right) \tag{4-3}$$

By rearranging equation 4-3,

$$2\zeta = \sqrt{\frac{R_1C_1}{R_2C_2}} + \sqrt{\frac{R_2C_2}{R_1C_1}} + (1-A)\sqrt{\frac{R_1C_2}{R_2C_1}} \tag{4-4}$$

Figures 4-4 through 4-6 are three examples of the frequency response which is attainable with this filter. The natural frequency, ω_n, has been shifted for each of the three figures, and the eight curves presented on each figure are the amplifier gains which correspond to a specific damping coefficient, zeta.

When substituting into equation 4-4 the component values that are associated with figure 4-4, it is found that:

$A = 3-2\zeta$

From this the following table is obtained:

ζ =	0.0	0.1	0.2	0.25	0.3	0.4	0.5	0.6
A =	3.0	2.8	2.6	2.5	2.4	2.2	2.0	1.8

The substitution of the component values associated with this figure into equation 4-2 results in the natural frequency ω_n being equal to 3.0. By examining figure 4-4, it is seen that the computed values of ζ and the amplifier gain 'A' associated with the desired values of zeta are in agreement with the corresponding curves that have been plotted in figure 4-4.

By applying this procedure to the other two figures, for figure 4-5 where $\omega_n = 10$:

ζ = 0.0	0.1	0.2	0.25	0.3	0.4	0.5	0.6
A = 3.5	3.3	3.1	3.0	2.9	2.7	2.5	2.3

and for figure 4-6 where $\omega_n = 100$:

ζ = 0.0	0.1	0.2	0.25	0.3	0.4	0.5	0.6
A = 3.0	2.8	2.6	2.5	2.4	2.2	2.0	1.8

The result of further investigation in this section was the constant bandwidth curve of figure 4-7. While this figure provides the values of R_1 and the amplifier 'A' necessary to maintain a constant magnitude of the transfer function at the specified frequency, no information is presented with respect to the value of zeta which is associated with each of these values. Of particular interest is the fact that the value of the natural frequency is continually changed as R_1 is varied which can be readily verified from equation 4-2. Thus the information obtained by examining the constant bandwidth curves of figure 4-7 is of little assistance in the design of this section.

Since the purpose of the entire network is to provide a frequency response with a high Q, a formulation of graphs consisting of constant zeta curves should prove desirable. Considering equation 4-4, two discrete representations can be generated when (1) $R_1 = R_2$ or (2) $C_1 = C_2$. For the case when $R_1 = R_2$

$$A = \frac{C_1}{C_2} - 2\zeta\sqrt{\frac{C_1}{C_2}} + 2$$

and for $C_1 = C_2$

$$A = \frac{R_2}{R_1} - 2\zeta\sqrt{\frac{R_2}{R_1}} + 2.$$

Figure 4-8 shows the constant zeta curves which result from either of the above equations when the amplifier gain "A" is the abcissa and R_2/R_1 or C_1/C_2 is the ordinate. The significance of these curves lies in the fact that they can be applied regardless of what value of natural frequency ω_n is desired, since the only specifications are the relationships which exist between C_1 and C_2, or between R_1 and R_2. When entering this figure with the component values associated with figures 4-4 through 4-6, observe that the results do in fact correspond. Thus the constant zeta curves represented by figure 4-8 do provide useful information for the design of this section.

4.3. For the second section of the double tuned filter shown in figure 4-3, from equation 7 of Appendix A the transfer function is

$$T_2(s) = \frac{BR_4C_3s(1+R_6C_6s)}{1+s(R_3C_3+R_5C_5+R_6C_6+R_4C_3+R_4C_5+(1-B)R_5C_6+(1-B)R_4C_6)} \tag{4-5}$$

$$+s^2(R_3R_5C_3C_5+R_3R_6C_3C_6+R_3R_4C_3C_5+R_4R_6C_5C_6+R_4R_6C_3C_6$$

$$+R_4R_5C_3C_5+R_5R_6C_5C_6+(1-B)R_4R_5C_3C_6+(1-B)R_3R_5C_3C_6$$

$$+(1-B)R_3R_4C_3C_6)$$

$$+s^3(R_4R_5R_6C_3C_5C_6+R_3R_5R_6C_3C_5C_6+R_3R_4R_6C_3C_5C_6)$$

By examining the combination of elements present in the input portion of this section, it is seen that they are in an array similar to that of a bandpass filter. The frequency responses shown in figures 4-9 and 4-10 confirm that this section does in fact represent a form of a bandpass filter. Of particular interest is the marked differences which are present in the two figures. Figure 4-9 has a very pronounced peaking which is the desirable condition to attain a high Q, while the response of figure 4-10 is much broader, rising and falling at a rate of 20 db per decade. Since it is the high Q which is desired for the overall network, only figure 4-9 will be examined. Using the component values that generated the family of curves of this figure,

$$T_2(s) = \frac{0.01Bs(1 + 0.1s)}{1 + s(0.51-0.15B) + s^2(0.147-0.011B) + 0.00155s^3}$$

or rearranging:

$$T_2(s) = \frac{0.645Bs(s + 10)}{s^3 + s^2(95-7.18B) + s(329-96.75B) + 645}$$

Now considering the curve corresponding to the amplifier gain 'B' equal to 3.0, the transfer function becomes:

$$T_2(s) = \frac{1.935\ s(s + 10)}{s^3 + 73.56s^2 + 38.74s + 645}$$

Extracting one of the roots from the denominator,

$$T_2(s) = \frac{1.935\ s(s + 10)}{(s + 73.142)(s^2 + 0.408s + 8.87)}$$

By equating

$$s^2 + 0.408s + 8.87 = s^2 + 2\zeta\omega_n s + \omega_n^2$$

from which:

$$\omega_n = \sqrt{8.87} = 2.97 \qquad \zeta = (0.408)/(2)(2.97) = 0.0688$$

The values of these poles are readily confirmed when examining figure 4-9. The peaking occurs at omega equal to 3 which is the case for complex conjugate roots as two of the poles. An additional 20 db drop occurs in the vicinity of omega equal to 70 which corresponds to the real pole at s equal to 73.142.

4.4. For section 3 of the double tuned filter, the high pass filter section, the 3 db down frequency is easily determined by equation 8 of Appendix A and no additional amplification is necessary.

4.5. To complete the investigation of the double tuned filter, the three individual sections will be combined. For this illustration a resonant peak located at omega equal to 3 will be examined. Using the component values which resulted in figures 4-4 and 4-9 and a 3 db down frequency for the high pass section located at omega equal to 3, the transfer function for the entire network can be derived by the multiplication of the three individual transfer functions; i.e.,

$$T(s) = T_1(s)\ T_2(s)\ T_3(s)$$

The two amplifier gains will be retained as variables in deriving the combined transfer function.

Using these element values, the combined transfer function becomes:

$$T(s) = \frac{0.03333ABs^2+0.03663ABs^3+0.00333ABs^4}{1+s(2.083-A-0.15B)+s^2(1.353-0.1783A-0.1075B+0.05AB)+s^3(0.3815-0.0808A-0.02445B+0.00625AB)+s^4(0.111-0.01208A-0.00188B+0.00042AB)+s^5(0.02342-0.00042A-0.00004B)+0.00004s^6}$$

Figures 4-11 through 4-13 are the frequency responses obtained when B the amplifier gain of section 2 has the values 2.5, 2.0 and 1.5 respectively, and the section 1 amplifier gain A varies over the range of 1.0 to 3.0. In each figure the peak response occurs for the amplifier gain A equal to 3.0. For these three figures observe that for figure 4-11 there is a 25 db drop per octave, for figure 4-12 the drop is 30 db per octave, and for figure 4-13 a 40 db drop per octave is achieved. These responses are the ones desired for this high Q double tuned filter.

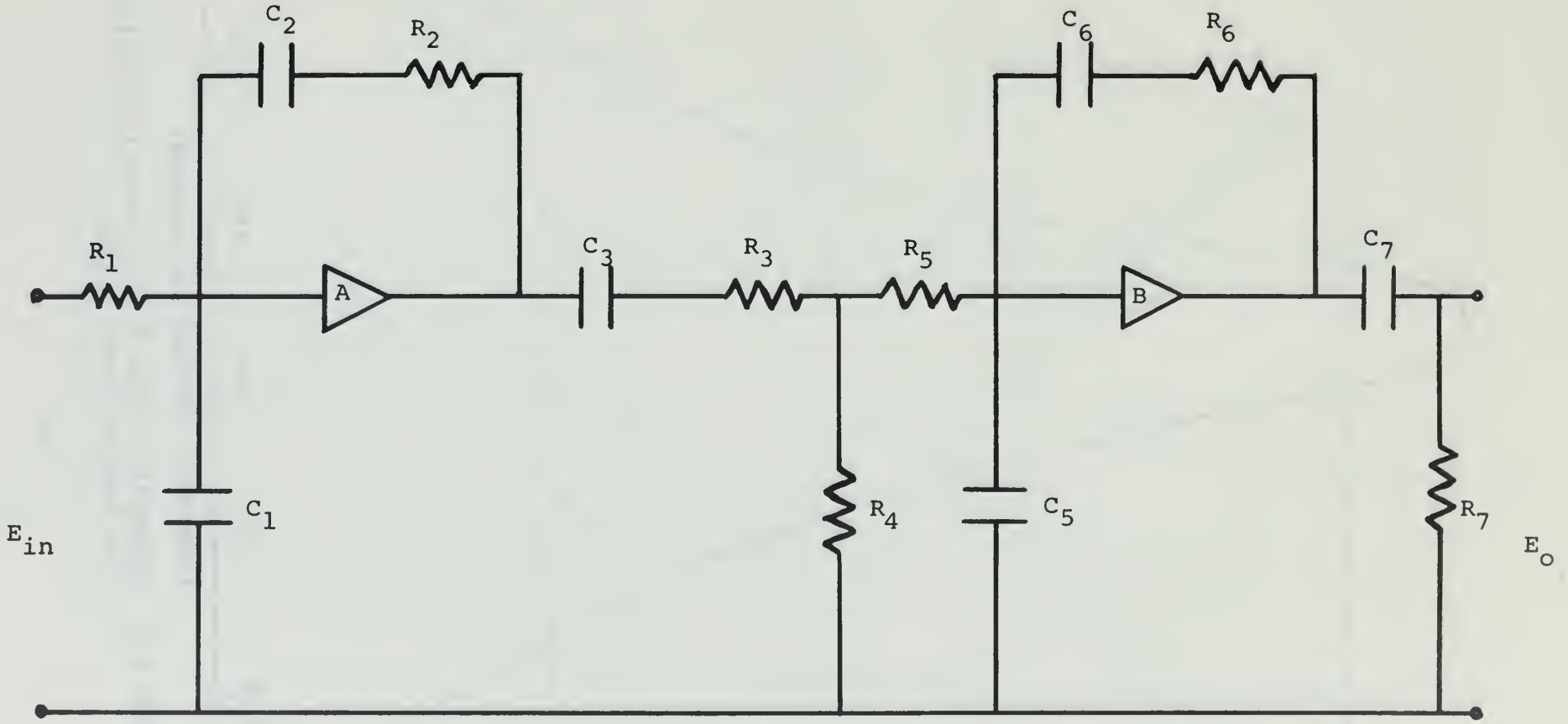

Figure 4-1. Circuit Diagram, Double Tuned Filter

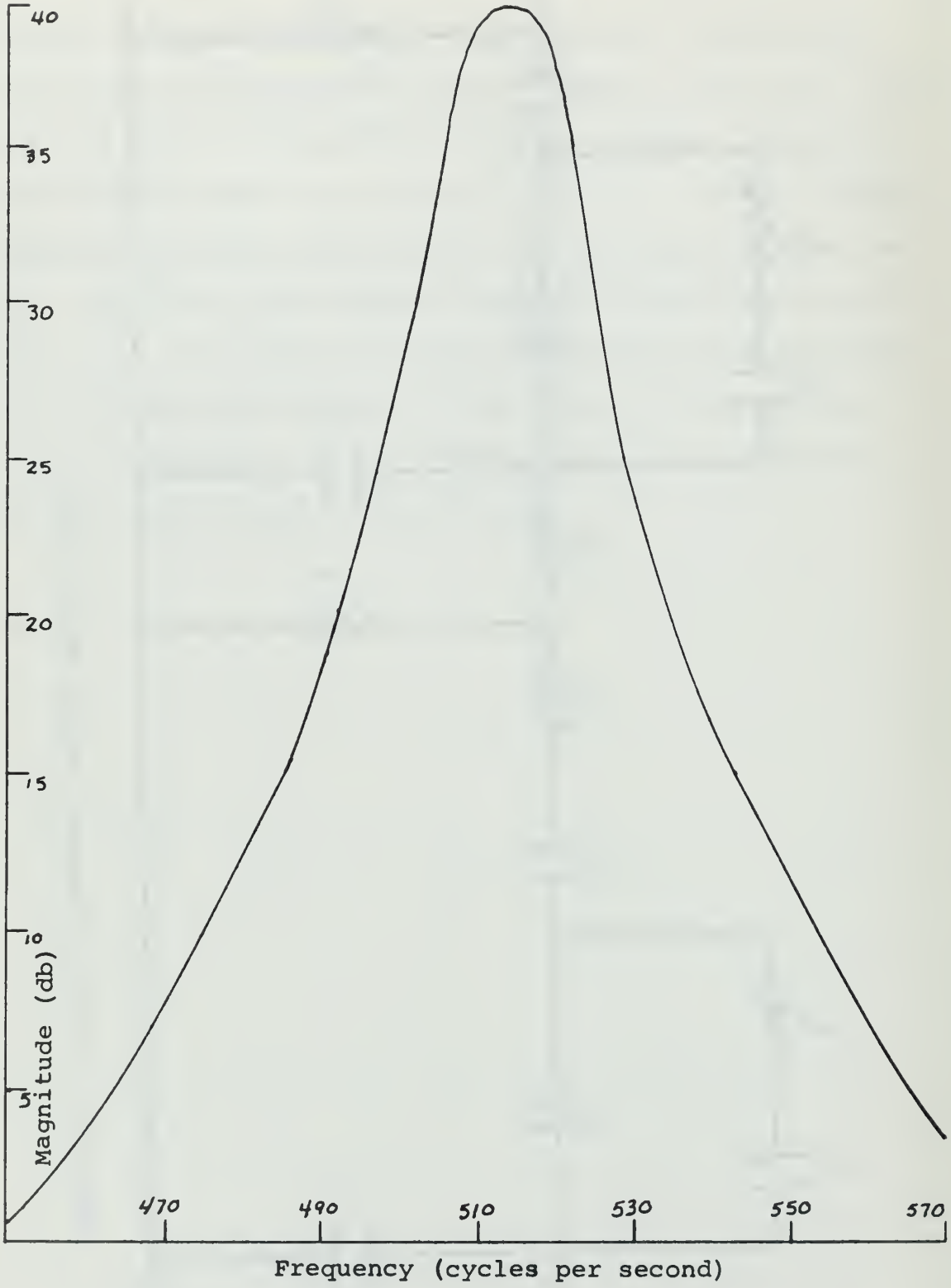

Figure 4-2. Example of the High Q Associated with the Double Tuned Filter

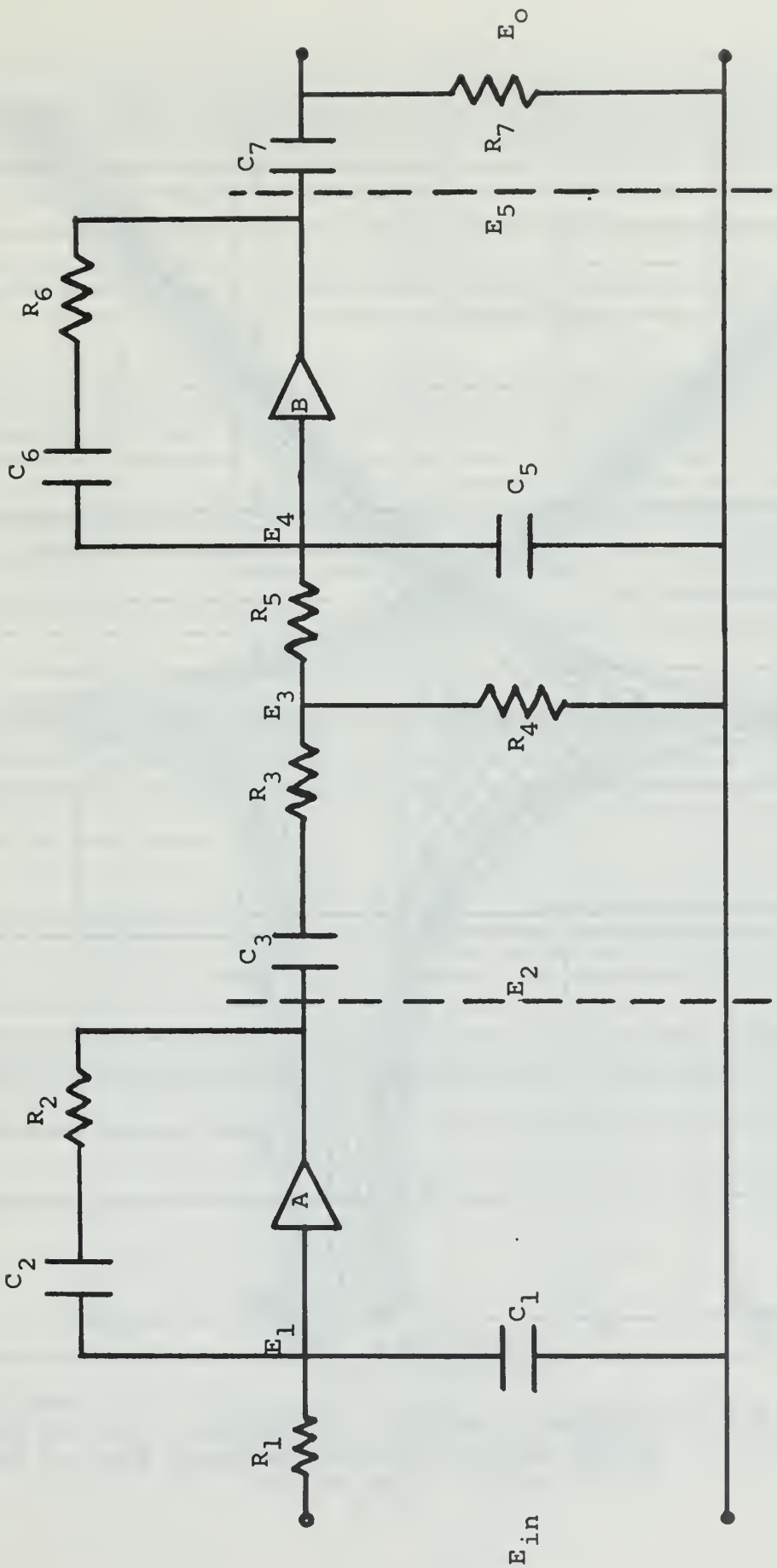

Figure 4-3. Circuit Diagram Representing the Three Independent Sections of the Double Tuned Filter

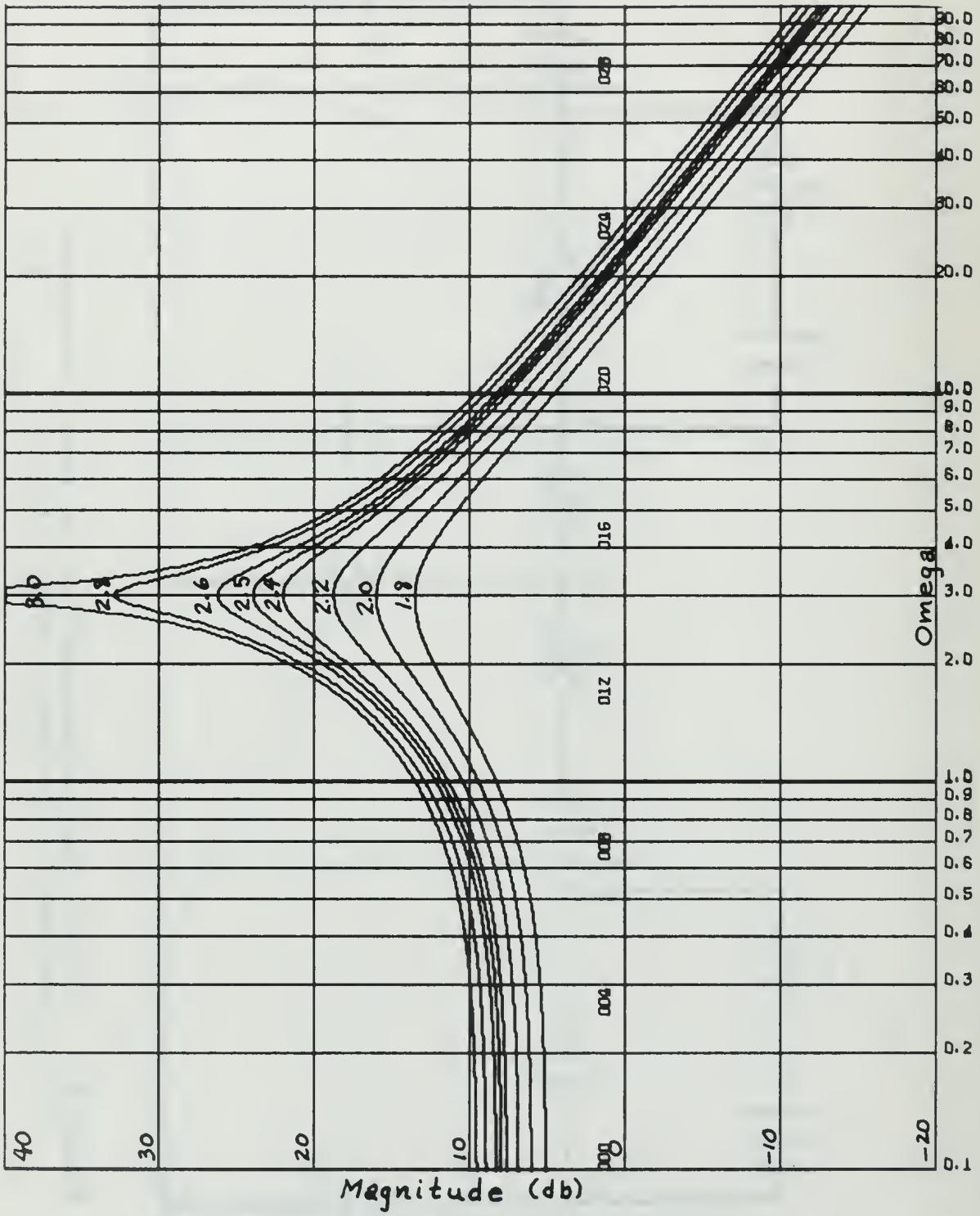

Figure 4-4. Frequency Response of Section 1 of the Double Tuned Filter with the Resonant Peak at Omega = 3. $C_1=C_2=1$ $R_1=R_2=0.333$

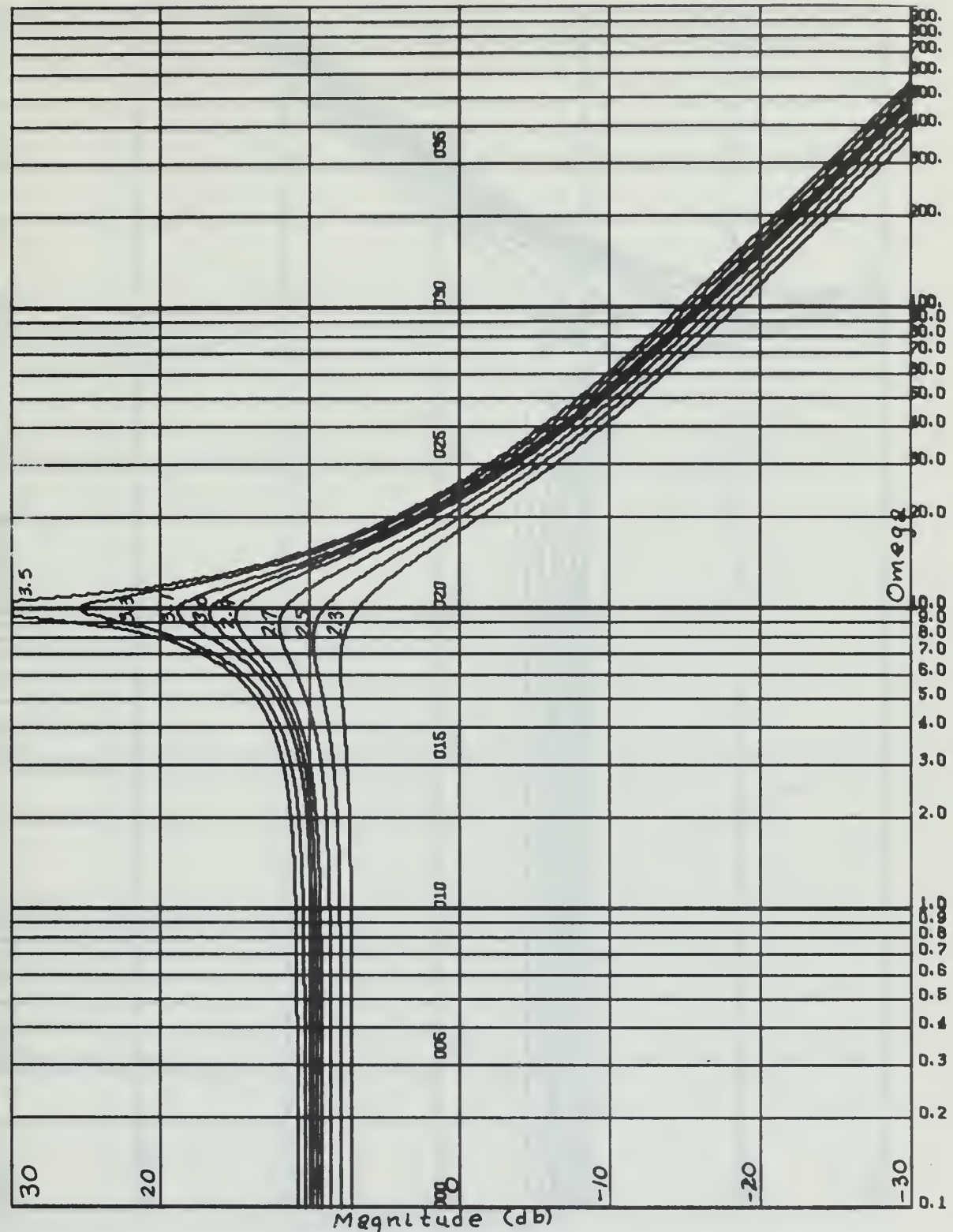

Figure 4-5. Frequency Response of Section 1 of the Double Tuned Filter with the Resonant Peak at Omega = 10. $R_1 = 0.1$ $R_2 = 0.05$ $C_1 = 2$ $C_2 = 1$

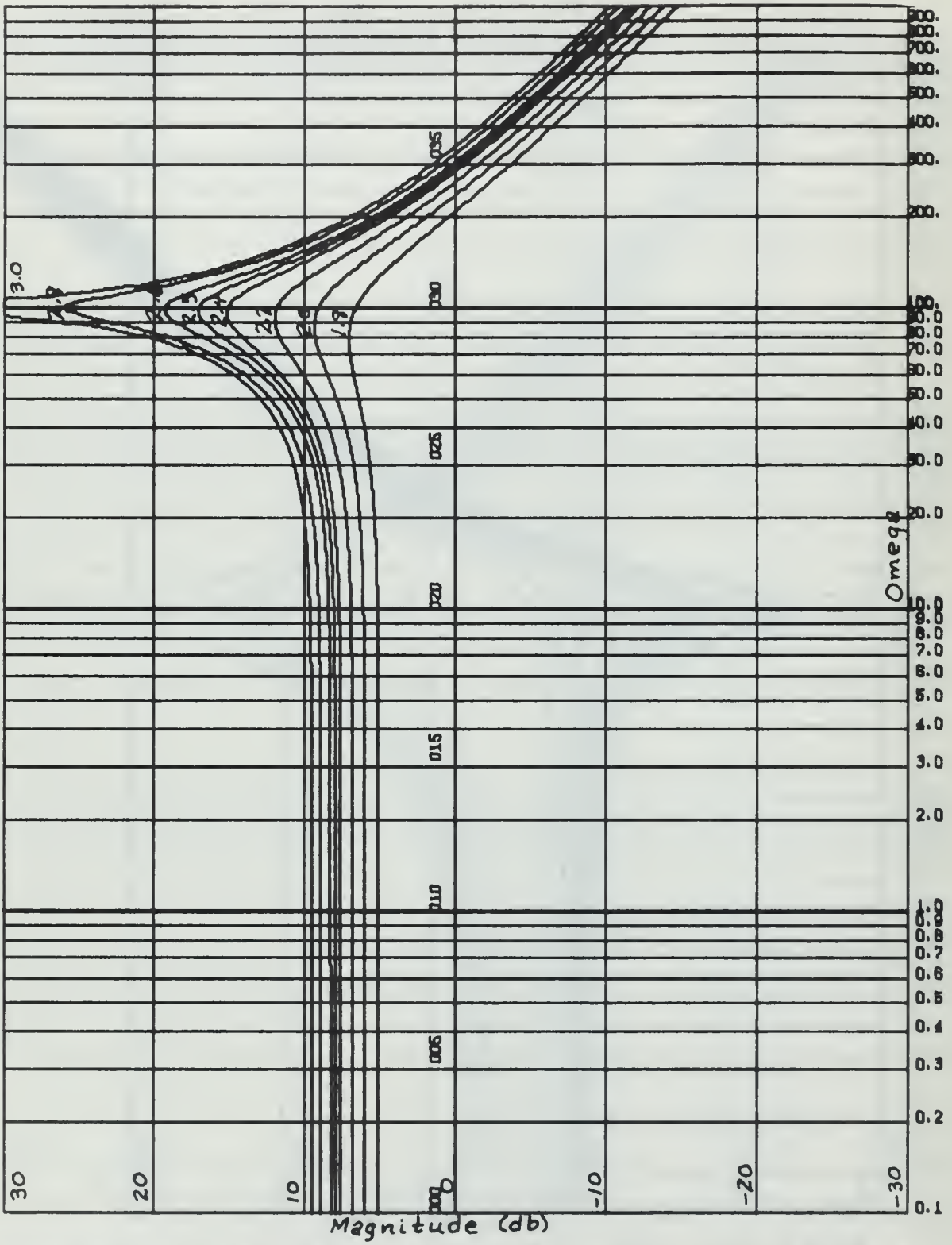

Figure 4-6. Frequency Response of Section 1 of the Double Tuned Filter with the Resonant Peak at Omega = 100. $R_1 = R_2 = 0.1$ $C_1 = C_2 = 0.1$

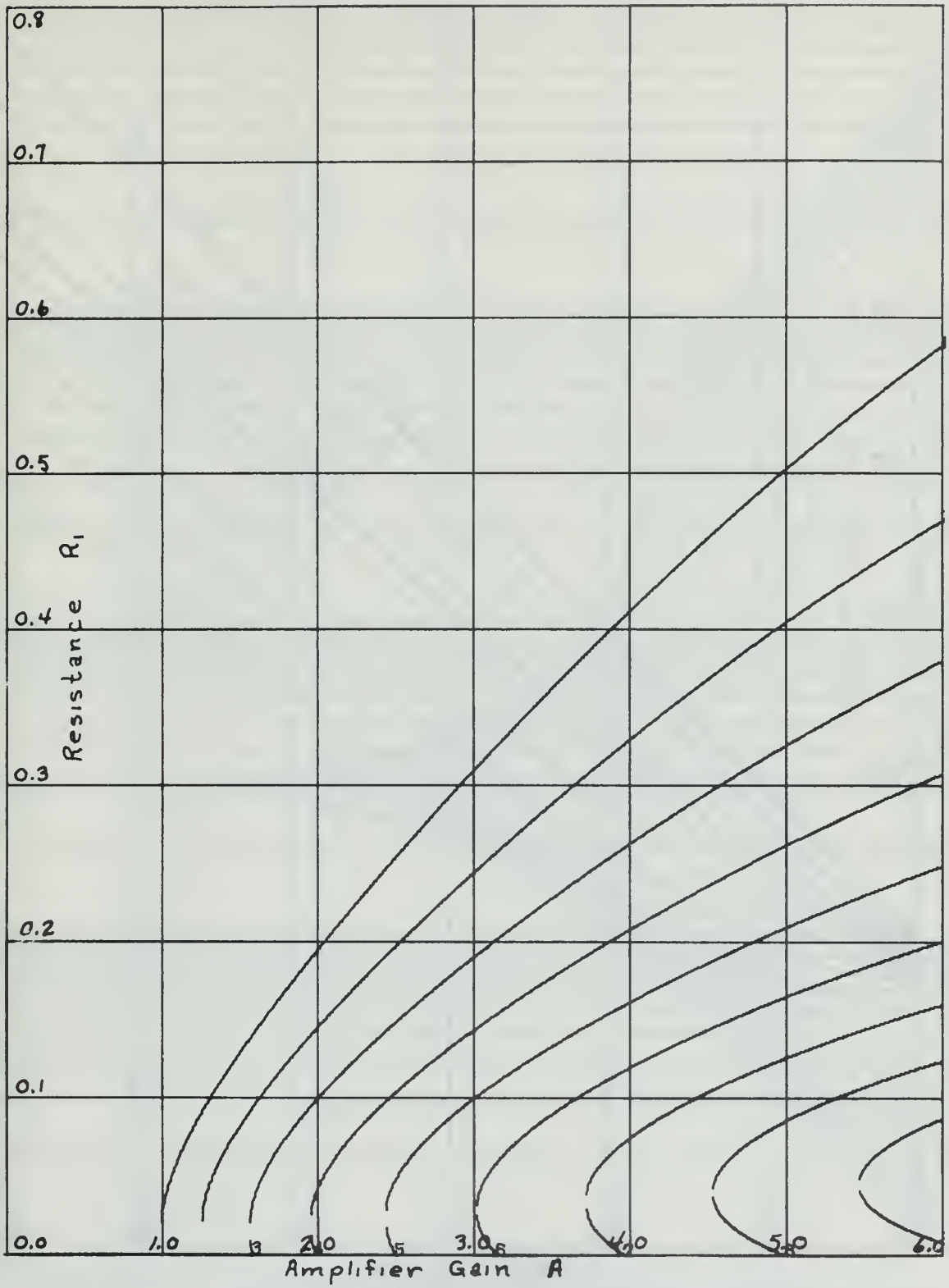

Figure 4-7. Constant Bandwidth Curves of Section 1 of the Double Tuned Filter for Omega = 10

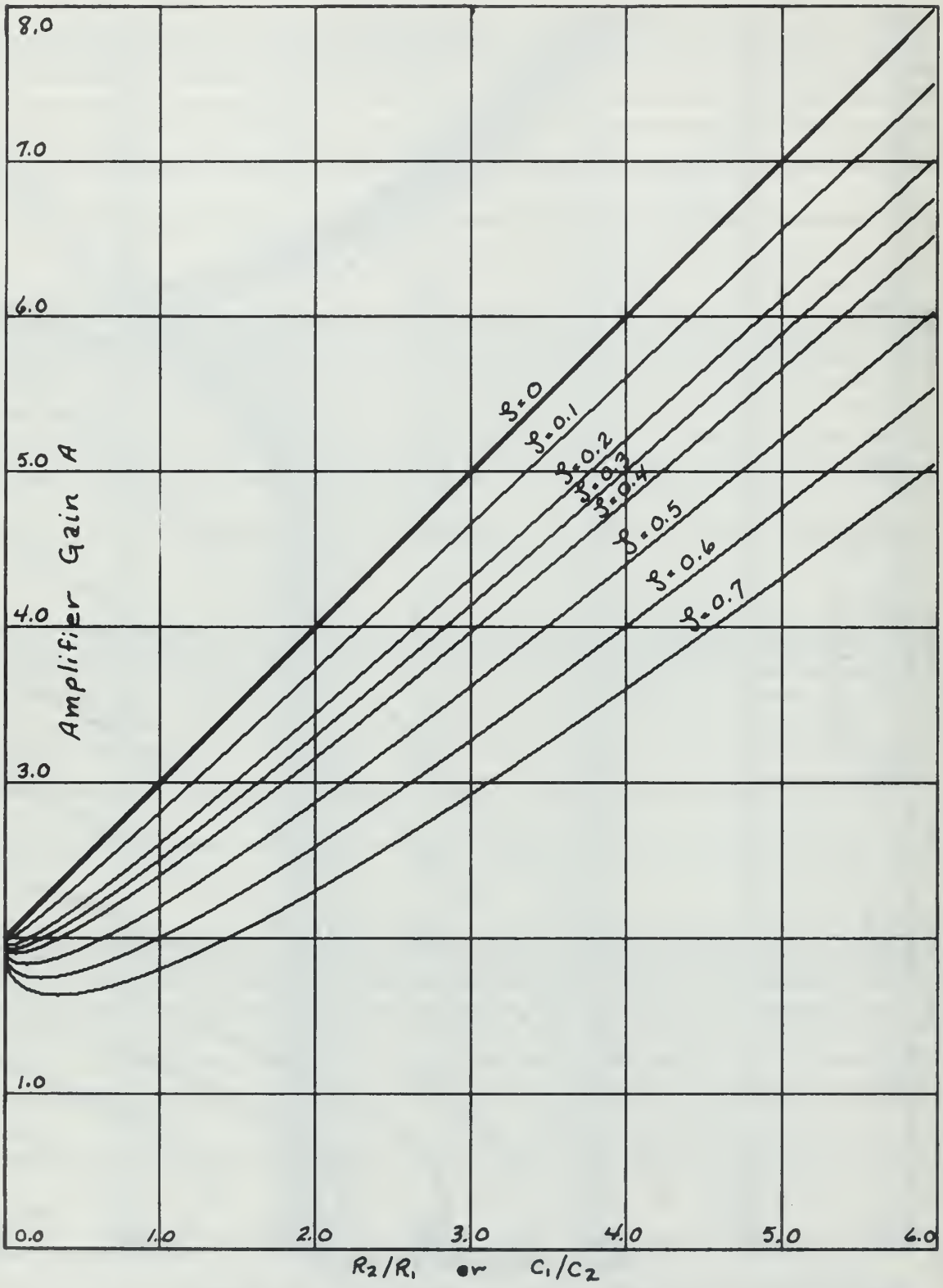

Figure 4-8. Constant Zeta Curves for Section 1 of the Double Tuned Filter

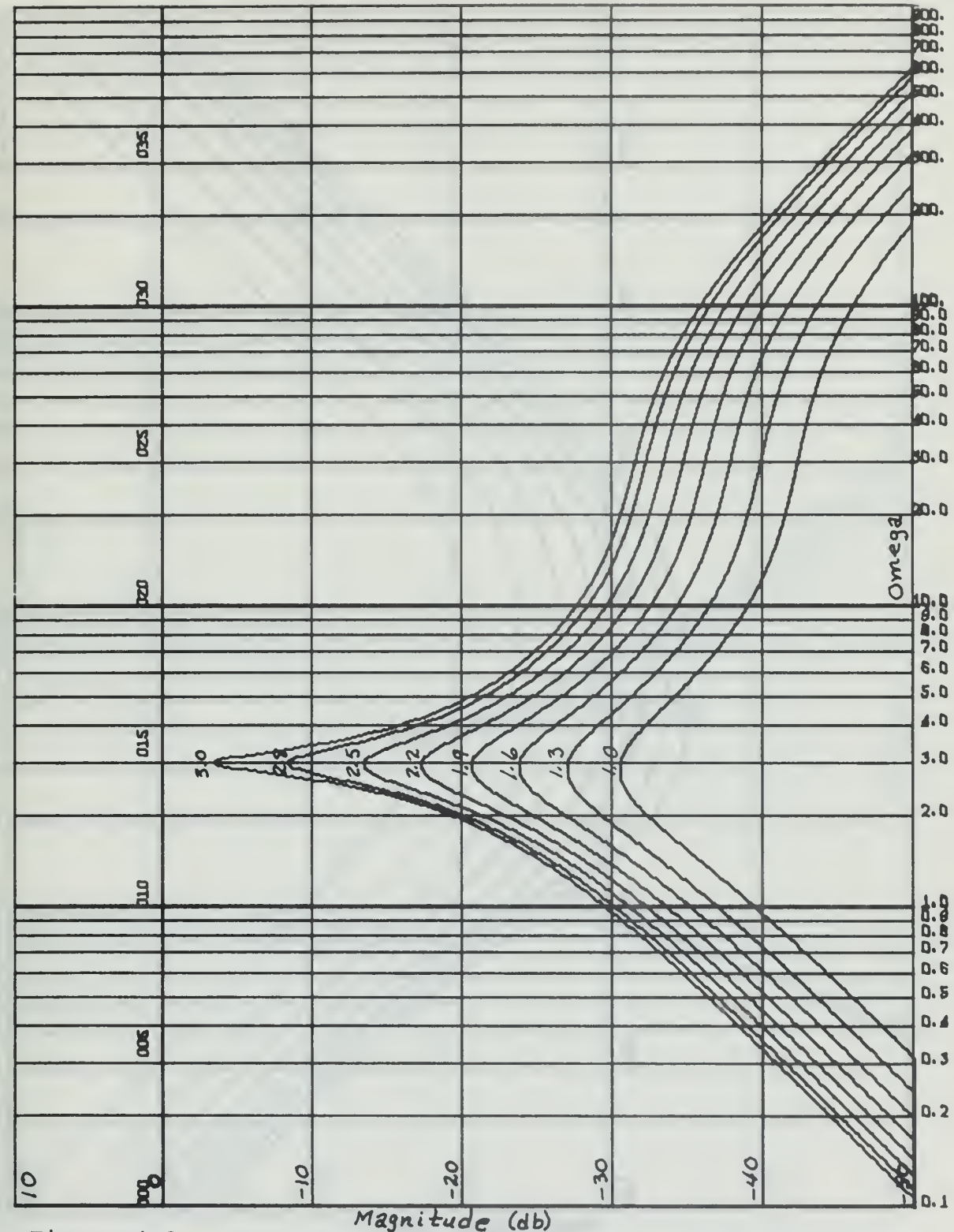

Figure 4-9. Frequency Response of Section 2 of the Double Tuned Filter with Two of the Poles Being Complex Conjugates. $R_3 = 1$ $R_4 = R_5 = 0.1$ $R_6 = 0.1$ $C_3 = 0.1$ $C_5 = C_6 = 1$

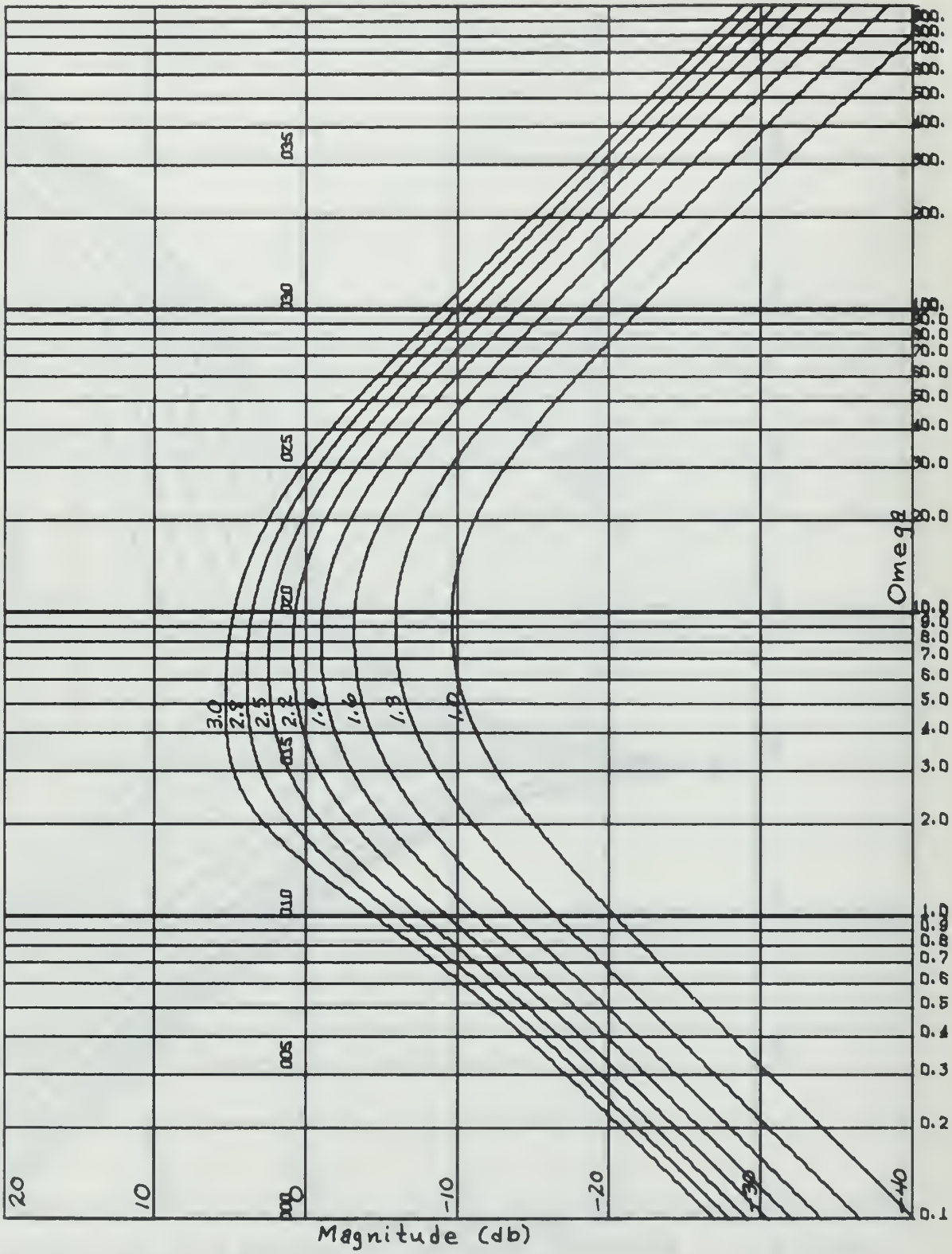

Figure 4-10. Frequency Response of Section 2 of the Double Tuned Filter with Three Real Poles.
$R_3 = R_5 = 0.05$ $R_4 = 0.1$ $R_6 = 1$ $C_3 = C_5 = C_6 = 1$

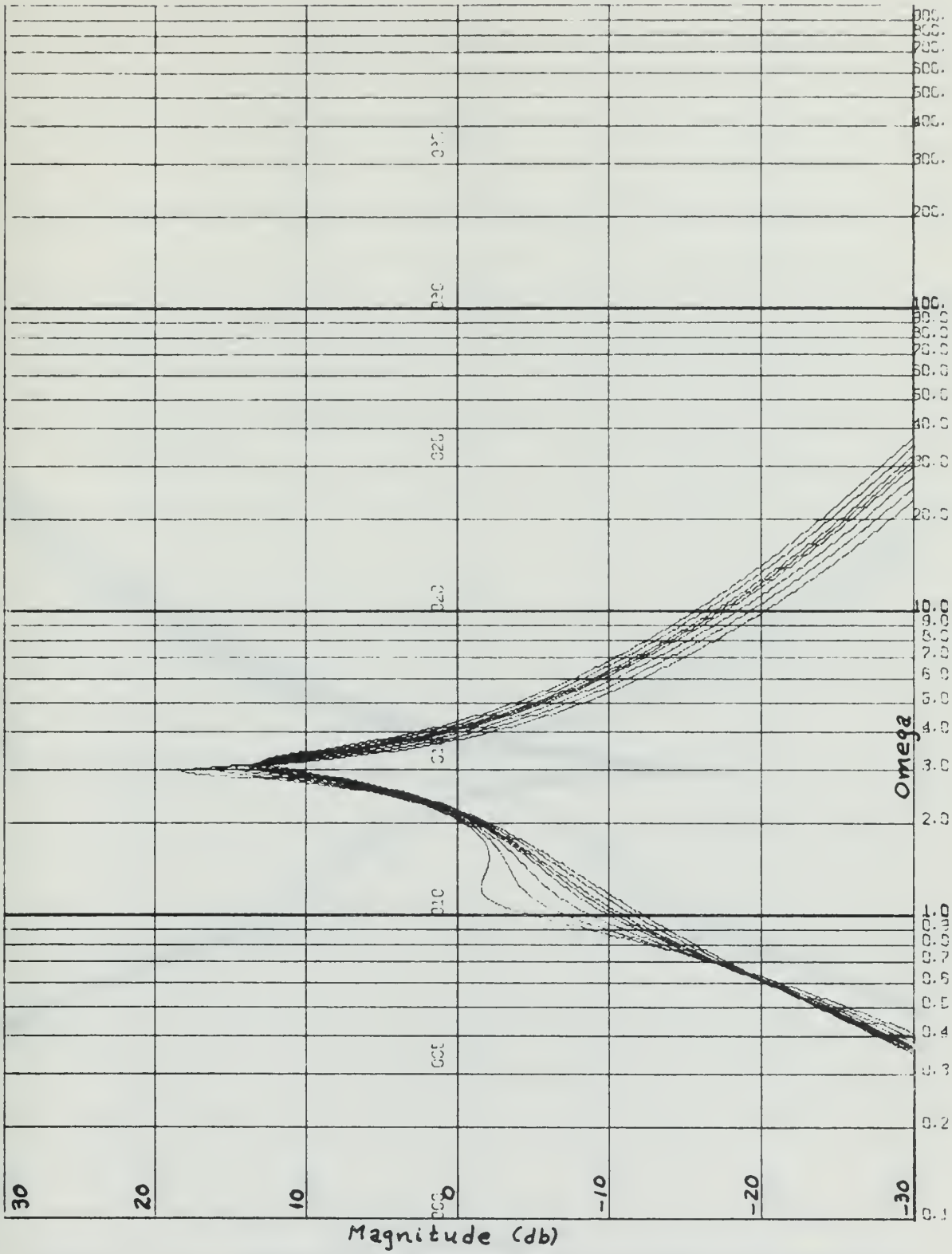

Figure 4-11. Frequency Response of the Double Tuned Filter with the Amplifier Gain of Section 2 Equal to 2.5

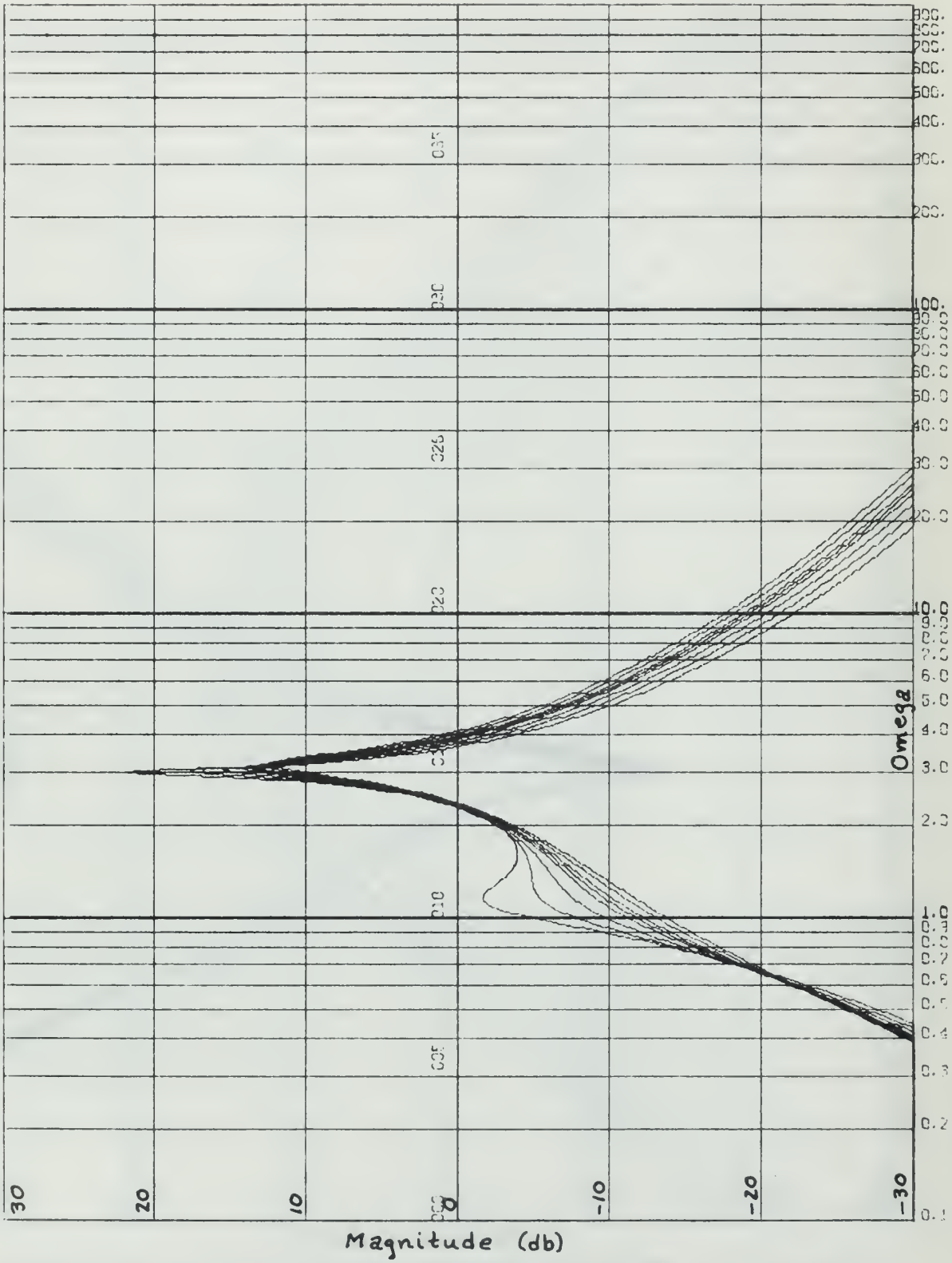

Figure 4-12. Frequency Response of the Double Tuned Filter with the Amplifier Gain of Section 2 Equal to 2.0

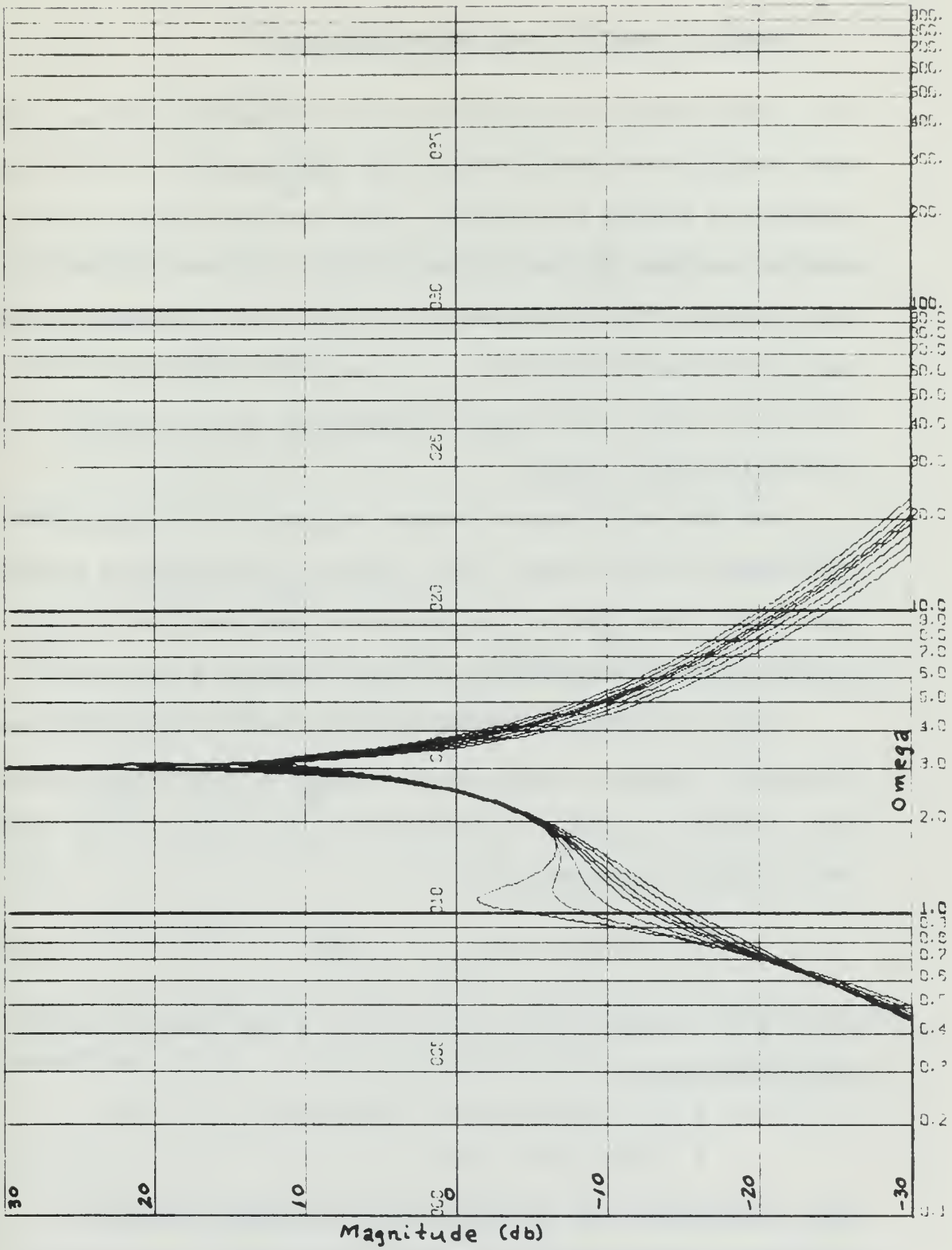

Figure 4-13. Frequency Response of the Double Tuned Filter with the Amplifier Gain of Section 2 Equal to 1.5

5. GENERAL COMMENTS AND RECOMMENDATIONS

5.1. Two different applications of parameter planes in network design were demonstrated for the design of the active parallel-T filter of section 3 and for the design of the active low pass filter of section 4. For the active parallel-T filter, the utilization of constant bandwidth curves was demonstrated while the utilization of constant zeta curves provided additional information for the design of the active low pass filter.

For the third order system represented by section 2 of the double tuned filter, two different but related techniques were investigated for possible applications of the parameter plane techniques in this network's design.

Since the desired result was to have a network whose frequency response represented a high Q, the first technique involved a general solution for the poles of the transfer function represented by

$$(s + a)(s^2 + 2\zeta\omega_n s + \omega_n^2) \qquad (5\text{-}1)$$

First the denominator of equation 4-5 was rearranged and put in the form

$$s^3 + bs^2 + cs + d$$

Then performing the multiplication of equation 5-1 and equating coefficients:

$$a + 2\zeta\omega_n = b$$

$$\omega_n^2 + 2\zeta a\omega_n = c$$

$$a\omega_n^2 = d$$

By performing the necessary operations on these equations it is possible to formulate independent relationships for a and ω_n. These are

$$\omega_n^6 - c\ \omega_n^4 + bd\ \omega_n^2 - d^2 = 0$$

and

$$a^3 - bda^2 + cda - d = 0$$

However, the formulation of an independent relationship for ζ resulted in the following two equations.

$$2\zeta\omega_n^3 + d = b\ \omega_n^2$$

and

$$\omega_n^3 + 2\zeta d = c\ \omega_n$$

Since the elimination of ω_n from these two equations is not possible, and ω_n is not a function which is independent of b, c, and d, an independent relationship for ζ could not be found.

With the inability to formulate an independent relationship for zeta, which is the most important factor in

the determination of the roots which will give the desired high Q, a second technique was employed. From (4),

$$s^3 + bs^2 + cs + 1 = (1+\omega_n{}^2 s)\left(1+ \frac{2\zeta s}{\omega_n} + \frac{s^2}{\omega_n{}^2}\right)$$

$$= s^3 + s^2\left(2\zeta\omega_n + \frac{1}{\omega_n{}^2}\right) + s\left(\frac{2\zeta}{\omega_n} + \omega_n{}^2\right) + 1$$

Using this equation and the relationship that

$$\frac{a_o}{s^3 + a_2 s^2 + a_1 s + a_o} = \frac{1}{s^3 + bs^2 + cs + 1}$$

where

$$b\omega_o = a_2$$

$$c\omega_o{}^2 = a_1$$

$$\omega_o{}^3 = a_o$$

an attempt was made to determine whether the results shown in (4) could be achieved. This investigation also resulted in the inability to formulate the desired independent relationships.

5.2. Recommendations

5.2.1. It is recommended that further study be given to the formulation of adequate and satisfactory parameter plane representations for third order systems.

BIBLIOGRAPHY

1. Thaler, G. J., Siljak, D. D., and Dorf, R.C., "Algebraic Methods for Dynamic Systems", NASA Contractor Report, NASA CR-617, November 1966.

2. Hollister, F. H., "Network Analysis and Design by Parameter Plane Techniques", Ph.D. Dissertation, Naval Postgraduate School, Monterey, California, 1965.

3. Nakagawa, G. R., "Parameter Plane Techniques for Active Filter Systems", M.S. Thesis, Naval Postgraduate School, Monterey, California, December, 1966.

4. Brown, J. M., "Fundamental Impulse Response Characteristics of Third Order Zero Displacement Error and Third Order Zero Velocity Error Control Systems", Technical Note DAG. 5, Welsh College of Advanced Technology, March, 1967.

APPENDIX A

Derivations of the transfer functions for the Double Tuned Filter.

The transfer function for section 1 of figure 4-3 is:

$$\frac{E_{in}}{R_1} - \frac{E_1}{R_1} - E_1C_1s + \frac{E_2C_2s}{1+R_2C_2s} - \frac{E_1C_2s}{1+R_2C_2s} = 0 \qquad (1)$$

$$E_2 = AE_1 \qquad (2)$$

$$\frac{E_{in}}{R_1} + \frac{E_2C_2s}{1+R_2C_2s} = \frac{E_1}{R_1} + E_1C_1s + \frac{E_1C_2s}{1+R_2C_2s}$$

$$E_{in} + \frac{E_2R_1C_2s}{1+R_2C_2s} = E_1 + E_1R_1C_1s + \frac{E_1R_1C_2s}{1+R_2C_2s}$$

$$E_{in} + E_{in}R_2C_2s + E_2R_1C_2s = E_1+E_1R_2C_2s + E_1R_1C_1s + E_1R_1R_2C_1C_2s^2 + E_1R_1C_2s$$

$$AE_{in} + AE_{in}R_2C_2s = E_2\left[1 + s(R_1C_1+ R_2C_2 + (1-A)R_1C_2 + R_1C_1R_2C_2s^2\right]$$

$$T_1(s) = \frac{E_2(s)}{E_{in}(s)} = \frac{A(1 + R_2C_2s}{1 + s[R_1C_1+ R_2C_2+ (1-A)R_1C_2]+ R_1C_1R_2C_2s^2}$$

$$T_1(s) = \frac{(A/R_1C_1)(s + (1/R_2C_2))}{s^2+ s(R_1C_1 + R_2C_2+ (1-A)R_1C_2)/R_1C_1R_2C_2+(1/R_1C_1R_2C_2)} \qquad (3)$$

For section 2 of figure 4-3 the transfer function is:

$$\frac{E_2 - E_3}{R_3 + 1/C_3 s} - \frac{E_3}{R_4} + \frac{E_4 - E_3}{R_5} = 0 \qquad (4)$$

$$\frac{E_3 - E_4}{R_5} - E_4 C_5 s + \frac{E_5 - E_4}{R_6 + 1/C_6 s} = 0 \qquad (5)$$

$$E_5 = BE_4 \qquad (6)$$

Rearranging equation 4

$$\frac{E_2 C_3 s}{1+R_3 C_3 s} + \frac{E_4}{R_5} = \frac{E_3 C_3 s}{1+R_3 C_3 s} + \frac{E_3}{R_4} + \frac{E_3}{R_5}$$

$$E_2 R_4 R_5 C_3 s + E_4 R_4 (1+R_3 C_3 s) = E_3 R_4 R_5 C_3 s + E_3 R_5 (1+R_3 C_3 s) + E_3 R_4 (1+R_3 C_3 s)$$

$$E_3 = \frac{E_2 R_4 R_5 C_3 s + E_4 R_4 (1+R_3 C_3 s)}{R_4 R_5 C_3 s + R_5 (1+R_3 C_3 s) + R_4 (1+R_3 C_3 s)} \qquad (4a)$$

for equation (5)

$$\frac{E_3}{R_5} = \frac{E_4}{R_5} + E_4 C_5 s - \frac{E_5 C_6 s}{1+R_6 C_6 s} + \frac{E_4 C_6 s}{1+R_6 C_6 s}$$

$$E_3 = \frac{E_4 (1+R_6 C_6 s) + E_4 R_5 C_5 s (1+R_6 C_6 s) + E_4 R_5 C_6 s - E_5 R_5 C_6 s}{1 + R_6 C_6 s} \qquad (5a)$$

By equating equations (4a) and (5a) and cross multiplying

$$(E_2 R_4 R_5 C_3 s + E_4 R_4 (1+R_3 C_3 s))(1+R_6 C_6 s) =$$

$$= (R_4 R_5 C_3 s + R_5 (1+R_3 C_3 s) + R_4 (1+R_3 C_3 s))(E_4 (1+R_6 C_6 s)$$

$$+ E_4 R_5 C_5 s (1+R_6 C_6 s) + E_4 R_5 C_6 s - E_5 R_5 C_6 s)$$

$$\left[E_2R_4R_5C_3s + E_4R_4 + E_4R_4R_3C_3s\right]\left[1 + R_6C_6s\right] =$$

$$= \left[R_4R_5C_3s + R_5 + R_5R_3C_3s + R_4 + R_4R_3C_3s\right] \times$$

$$\left[E_4 + E_4R_6C_6s + E_4R_5C_5s + E_4R_5R_6C_5C_6s^2 + E_4R_5C_6s - E_5R_5C_6s\right]$$

$$B\,E_2\left[R_4R_5C_3s + R_4R_5R_6C_3C_6s^2\right] = E_5R_5$$

$$+ E_5\left[R_4R_5C_3 + R_5R_6C_6 + R_5^2C_5 + R_5^2C_6 - B\,R_5^2C_6 + R_3R_5C_3\right.$$

$$\left. + R_4R_5C_5 + R_4R_5C_6 - B\,R_4R_5C_6\right]s$$

$$+ E_5\left[R_4R_5R_6C_3C_6 + R_4R_5^2C_3C_5 + R_4R_5^2C_3C_6 - B\,R_4R_5^2C_3C_6\right.$$

$$+ R_5^2R_6C_5C_6 + R_3R_5R_6C_3C_6 + R_3R_5^2C_3C_5 + R_3R_5^2C_3C_6$$

$$- B\,R_3R_5^2C_3C_6 + R_4R_5R_6C_5C_6 + R_3R_4R_5C_3C_5 + R_3R_4R_5C_3C_6$$

$$\left. - B\,R_3R_4R_5C_3C_6\right]s^2$$

$$+ E_5\left[R_4R_5^2R_6C_3C_5C_6 + R_3R_5^2R_6C_3C_5C_6 + R_3R_4R_5R_6C_3C_5C_6\right]s^3$$

$$T_2(s) = E_5(s)/E_2(s) =$$

$$\frac{BR_4C_3s(1 + R_6C_6s)}{1 + s(R_4C_3 + R_6C_6 + R_5C_5 + R_5C_6 - BR_5C_6 + R_3C_3 + R_4C_5 + R_4C_6 - BR_4C_6) +}$$

$$+ s^2(R_4R_6C_3C_6 + R_4R_5C_3C_5 + R_4R_5C_3C_6 - BR_4R_5C_3C_6$$

$$+ R_5R_6C_5C_6 + R_3R_6C_3C_6 + R_3R_5C_3C_5 + R_3R_5C_3C_6$$

$$- BR_3R_5C_3C_6 + R_4R_6C_5C_6 + R_3R_4C_3C_5 + R_3R_4C_3C_6$$

$$- BR_3R_4C_3C_6) + s^3(R_4R_5R_6C_3C_5C_6 + R_3R_5R_6C_3C_5C_6 + R_3R_4R_6C_3C_5C_6)$$

(7)

$$T_2(s) = \frac{BR_4C_3s(1 + R_6C_6s)}{1 + s(R_3C_3 + R_5C_5 + R_6C_6 + R_4C_3 + R_4C_5 + (1-B)R_5C_6 + (1-B)R_4C_6)}$$

$$+ s^2(R_3R_5C_3C_5 + R_3R_6C_3C_6 + R_3R_4C_3C_5 + R_4R_6C_5C_6 + R_4R_6C_3C_6$$

$$+ R_4R_5C_3C_5 + R_5R_6C_5C_6 + (1-B)R_4R_5C_3C_6 + (1-B)R_3R_5C_3C_6$$

$$+ (1-B)R_3R_4C_3C_6)$$

$$+ s^3(R_4R_5R_6C_3C_5C_6 + R_3R_5R_6C_3C_5C_6 + R_3R_4R_6C_3C_5C_6)$$

For section 3 of figure 4-3 the transfer function is:

$$T_3(s) = \frac{s}{s + 1/RC} \tag{8}$$

INITIAL DISTRIBUTION LIST

		No. Copies
1.	Defense Documentation Center Cameron Station Alexandria, Virgina 22314	20
2.	Library Naval Postgraduate School Monterey, California 93940	2
3.	Commander, Naval Ordnance Systems Command Dept. of Navy Washington, D.C. 20360	1
4.	Professor G. J. Thaler Dept. of Electrical Engineering Naval Postgraduate School Monterey, California 93940	6
5.	LT Ronald C. Funk c/o Ted Funk Route 2, Lena, Wisconsin 54139	2

UNCLASSIFIED
Security Classification

DOCUMENT CONTROL DATA - R & D

(Security classification of title, body of abstract and indexing annotation must be entered when the overall report is classified)

1 ORIGINATING ACTIVITY *(Corporate author)*

Naval Postgraduate School
Monterey, California 93940

2a. REPORT SECURITY CLASSIFICATION

UNCLASSIFIED

2b. GROUP

3 REPORT TITLE

DESIGN OF ACTIVE FILTER SYSTEMS USING PARAMETER PLANE TECHNIQUES

4. DESCRIPTIVE NOTES *(Type of report and, inclusive dates)*

M. S. Thesis - Electrical Engineering - 1968

5. AUTHOR(S) *(First name, middle initial, last name)*

Ronald C. FUNK
Lieutenant, United States Navy

6 REPORT DATE	7a. TOTAL NO. OF PAGES	7b. NO. OF REFS
December 1968	75	4

8a. CONTRACT OR GRANT NO.

b. PROJECT NO.

c.

d.

9a. ORIGINATOR'S REPORT NUMBER(S)

9b. OTHER REPORT NO(S) *(Any other numbers that may be assigned this report)*

10. DISTRIBUTION STATEMENT

Distribution of this document is unlimited.

11. SUPPLEMENTARY NOTES

12. SPONSORING MILITARY ACTIVITY

Naval Postgraduate School
Monterey, California 93940

13. ABSTRACT

Since parameter planes were introduced, considerable investigation has been conducted in proving that the results obtained by this method are in agreement with those obtained from various other proven techniques. Reseach undertaken in this paper illustrates methods by which parameter planes are useful in the design of electrical networks. The investigations were conducted on an active parallel-T filter, in which the utilization of the constant bandwidth curves are beneficial, and the high Q double tuned filter, where constant zeta curves aided in the design.

DD FORM 1 NOV 65 1473 (PAGE 1)
S/N 0101-807-6811

UNCLASSIFIED
Security Classification

A-31408

14 KEY WORDS	LINK A		LINK B		LINK C	
	ROLE	WT	ROLE	WT	ROLE	WT
Parameter Plane Techniques						
Active Parallel-T Filter						
Double Tuned Filter						